THESIS FOR THE DEGREE OF DOCTOR OF PHILOSOPHY

Microbial biofilm communities associated with degradation of sprayed concrete in subsea tunnels

SABINA KARAČIĆ

Department of Architecture and Civil Engineering
CHALMERS UNIVERSITY OF TECHNOLOGY
Gothenburg, Sweden 2021

Microbial biofilm communities associated with degradation of sprayed concrete in subsea tunnels

SABINA KARAČIĆ

Doktorsavhandlingar vid Chalmers tekniska högskola
Ny serie nr 5027
ISSN 0346-718X

Department of Architecture and Civil Engineering
Chalmers University of Technology
SE-412 96 Gothenburg
Sweden
Telephone + 46 (0)31-772 1000

Chalmers Reproservice
Gothenburg, Sweden 2021

SABINA KARAČIĆ
Department of Architecture and Civil Engineering
Chalmers University of Technology

ABSTRACT

Deterioration of concrete leads to reduced structural strength implying high societal challenge with huge economic impact. In the Oslofjord subsea tunnel, complex microbial biofilm activity together with abiotic attack from saline groundwater are responsible for concrete matrix degradation and steel fiber corrosion. Previous research has revealed that microbial attack causes disintegration of cement paste matrix and thinning of sprayed concrete at rates varying from 0.5-10 mm/year in areas with leakages of saline groundwater. General knowledge about biodegradation of concrete infrastructures in marine environment is lacking and research in this area is therefore needed. A long-term study of biofilm microbial community composition and dynamics was performed between 2015-2020 in the Oslofjord subsea tunnel. Due to its complexity it was necessary to work multi-disciplinary, including studies of the microbial community structure by using advanced molecular techniques in combination with chemical analysis to get a comprehensive picture of the prevailing micro-environmental conditions within the biofilm. High throughput amplicon sequencing of 16S rRNA gene together with metagenomics shotgun sequencing revealed temporal dynamics in microbial community structure, and metabolic potential of biofilms in the Oslofjord tunnel. Water chemical analysis and microsensor measurements of oxygen and pH profiles within the biofilm were performed on-site to assess environmental conditions in the biofilms. Additionally, SEM microscopy together with XRD analyses were used to investigate concrete degradation beneath the biofilms over time. In parallel, a mesocosm experiment was performed over a period of 65 weeks to study the role of concrete material properties and fiber reinforcement for microbial colonization and composition. The long-term study preformed in the Oslofjord subsea tunnel revealed a complex microbial community involved in cement paste matrix degradation and steel fiber corrosion. The microbial communities at the different tunnel localities were composed of nitrogen converting bacteria, iron-oxidizing bacteria, sulfur oxidizing bacteria, heterotrophic aerobic bacteria, putative manganese-oxidizing bacteria and many microorganisms that could not be assigned to any function. Microsensor measurements showed relatively stable pH around 7-8 throughout the biofilm, whereas the dissolved oxygen profiles decreased with biofilm depth. Significant differences in community structure and richness between biofilms at the different tunnel locations were revealed with alpha and beta-diversity analysis. However, the microbial communities at the three sites shared many taxa. Pairwise comparisons suggested that deterministic factors were important for the assembly of the microbial communities of mature biofilms. Results from the mesocosms study indicate that stochastic factors were important during the initial colonization and time was the main factor which drives turnover in the biofilm communities on concrete material. Presence of steel fiber reinforcement was found to have a greater effect on the biofilm community composition than the surface roughness. The results obtained in this thesis help us to understand the complexity of microbial induced concrete deterioration and corrosion of steel fiber reinforcement observed in the subsea tunnel environments.

Keywords: microbially induced deterioration, biofilm, marine environment, concrete, subsea tunnels, surface structure, steel fibers, amplicon sequencing, metagenomics.

LIST OF PUBLICATIONS

This thesis is based on the following papers, which will be referred to in the text by their Roman numerals in bold:

I. **Karačić, S.**, Hagelia, P., Persson, F. and Wilén, B.-M. (2016) Microbial attack on subsea sprayed concrete. *International RILEM Conference on Microorganisms-Cementitious Materials Interactions*. Delft, Netherland: RILEM Publications SARL (peer-reviewed).

II. **Karačić, S.**, Wilén, B.-M., Suarez C., Hagelia, P., and Persson, F. (2018) Subsea tunnel reinforced sprayed concrete subjected to degradation harbours distinct microbial communities. *Biofouling. Vol. 34 Issue 10 p. 1161-1174.*

III. **Karačić, S.**, Hagelia, P., Suarez C., Hagelia, P., Persson, F., and Wilén, B.-M. Using metagenomics to understand sprayed concrete biodeterioration in a subsea road tunnel (manuscript).

IV. **Karačić, S.**, Persson, F., Modin, O., Hagelia P., and Wilén, B.-M. The role of time and surface type on the development of biofilm communities on concrete exposed to seawater (submitted).

The author of this thesis has made the following contribution:

Paper I: Contributed to the design of the study, sampling, data analysis and interpretation of the data (microbial community analysis and bioinformatics). Drafted and critically reviewed the manuscript.
Paper II: Contributed to the design of the study, sampling, data analysis and interpretation of the data (chemical analysis of water and biofilm samples, microsensor measurements, microbial community analysis and part of bioinformatics and statistical work). Drafted and critically reviewed the manuscript.
Paper III: Contributed to the design of experiment, performed part of the experimental work, preformed data analysis (chemical analysis, SEM, microbial community analysis and part of bioinformatics and statistical work). Drafted and critically reviewed the manuscript.
Paper IV: Contributed to the design of the study, sampling, data analysis and interpretation of data (chemical analysis of water, microbial community analysis and part of bioinformatics work). Drafted and critically reviewed the manuscript.

Other publications completed during the realization of this PhD:

- **Karačić, S.:** Microbially induced concrete degradation in subsea tunnels - Community structure of biofilms from sprayed reinforced concrete in the Oslofjord tunnel – Chalmers University of Technology. Gothenburg, Sweden. Licentiate thesis, 2018.

- Hagelia, P., **Karačić, S**., Haverkamp, THA., Persson, F. and Wilén, B.-M. (2021) Biodeterioration of sprayed concrete in subsea tunnels. Investigations into the role and nature of Mn–Fe biofilm over 17 years. *Book chapter: STAR 253-MCI*.RILEM. (accepted 2020, under final revision).

- **Karačić, S**., Hagelia, P., Haverkamp, THA., Persson, F. and Wilén, B.-M. (2018) Biodeterioration of reinforced sprayed concrete in subsea tunnels. Proceedings pro123: Final Conference of RILEM TC 253-MCI: Microorganisms-Cementitious Materials Interactions pp (209-221). Toulouse, France. Peer Reviewed-Proceeding. RILEM Publications S.A.R.L. e-ISBN: 978-2-35158-206-0. ISBN: 978-2-35158-209-1 (Volume1).

- **Karačić, S.**, Persson F., Hagelia, P., Wilén B.-M. (2017) Microbial biofilm induced degradation of sprayed reinforced concrete in the Oslofjord subsea tunnel in Norway. International Biodeterioration & Biodegradation Symposium (IBBS17), Manchester Metropolitan University, UK (Conference abstract).

ACKNOWLEDGEMENTS

The work of the thesis has been carried out at the Division of Water Environmental Technology, the Department of Architecture and Civil Engineering at the Chalmers University of Technology, within the project of Ferry free E39 funded by Norwegian Public Roads Administration (NPRA). I gratefully acknowledge financial support from the NPRA.

First of all, I would like to express my deep gratitude to my supervisors Britt-Marie Wilén, Frank Persson and Per Hagelia. Throughout my PhD, they have shared their vast knowledge and experience and without them this thesis would not have been completed. Given their level of commitment to the project, their understanding and support, I cannot think of anyone better to have as supervisors.

I would like to extend my gratitude to my co-authors to all the members of the Bioresource Lab research group. Special thanks to Carolina Suarez and Oskar Modin.

I am grateful to all my colleagues at the Division of Water Environmental Technology (WET) for creating such a nice and friendly working environment.

I would like to acknowledge to my family for your unconditional support and love without which I would not have come this far.

Finally, I owe special thanks to my husband Jesenko, for your endless encouragements and belief in me, and to my boy Isak Issa, for putting perspective to it all and reminding me of what is truly important. For all that and much more, thank you.

LIST OF ACRONYMS AND ABBREVIATIONS

ASOB: acidophilic sulfur-oxidizing bacteria
AOB: ammonia-oxidizing bacteria
DNA: deoxyribonucleic acid
DO: dissolved oxygen
EPS: extracellular polymeric substances
EDS: energy dispersive spectroscop
EDX: Energy Dispersive X-ray
IOB: iron oxidizing bacteria
IRB: iron reducing bacteria
MID: microbiologically induced deterioration
MICD: microbially induced concrete deterioration
MIC: microbiologically induced corrosion
MICC: microbially induced concrete corrosion
NCB: nitrogen converting bacteria
NGS next generation sequencing
NMDS: non-metric multi-dimensional scaling
NOB: nitrite-oxidizing bacteria
NSOB: neutrophilic sulfur-oxidizing bacteria
PCA: principal component analysis
PCR: polymerase chain reaction
SEM: scanning electron microscopy
SES: standard effect size
SRB: sulfate reducing bacteria
SOB: sulfur-oxidizing bacteria
TOC: total organic carbon
TSA: thaumasite sulfate attack
XRD: x-ray diffraction

Trivial names of minerals	*Formula*
Aragonite	$CaCO_3$
Brucite	$Mg(OH)_2$
Buserite (-Na)	$Na_4Mn_{14}O_{27}\cdot 21H_2O$
Calcium silicate hydrate (C-S-H)	$CaO - SiO_2 - H_2O$
Calcite	$CaCO_3$
Ettringite	$3CaO\cdot Al_2O_3\cdot 3CaSO_4\cdot 32H_2O$
Ferrihydrite	$Fe(OH)_3$
Gypsum	$CaSO_4\cdot 2H_2O$
Manganosite	MnO
Portlandite	$Ca(OH)_2$
Rhodochrosite	$MnCO_3$
Silica fume	$SiO_2 - xH_2O$
Thaumasite	$CaSiO_3\cdot CaCO_3\cdot CaSO_4\cdot 15H_2O$
Todorokite	Mn_6O_{12}

TABLE OF CONTENTS

1 Preface

This doctoral thesis is based on research performed at the Division of Water Environment Technology at the Department of Architecture and Civil Engineering, Chalmers University of Technology, between May 2015 and July 2021 under the supervision of Britt-Marie Wilén, Frank Persson and Per Hagelia. This research project was funded by the Norwegian Public Road Administration (NPRA) as part of the "Coastal highway route E39" programme.

1.1 Research motivation and scope of thesis

The overall goal of this thesis was to increase the understanding of the mechanisms behind biologically induced degradation of sprayed concrete and accelerated corrosion of steel fibers in subsea tunnels caused by biofilm development.

The specific objectives were to:

- Investigate the microbial biofilm composition associated with degradation of sprayed concrete and corrosion of steel fiber reinforcement in the Oslofjord subsea tunnel (**Paper I-III**);
- Assess the biofilm and water chemical composition (**Paper II and III**);
- Determine the micro-environmental conditions within the formed biofilm (**Paper II**);
- Investigate microbial succession and biofilm evolution on sprayed concrete in subsea tunnels in terms of both time and space (**Paper I-III**);
- Investigate microbial colonization and succession on concrete in a marine environment (**Paper IV**);
- Determine how concrete surface type, including surface roughness and presence or absence of steel fibers, affects biofilm microbial community composition (**Paper IV**);
- Asses the metabolic potential of the Oslofjord subsea tunnel biofilms **(Paper III)** and;
- Determine how the biofilm interacts with sprayed concrete surface and eventually deteriorates it (**Paper II-IV**).

The four papers comprise the following studies:

- **Paper I**: In this initial study, microbial community composition and diversity of selected biofilm samples from the Oslofjord tunnel were assessed. In order to find and select appropriate methodology for isolation and analysis of concrete microbial biofilms, two different DNA extraction methods were compared.
- **Paper II**: In this study, the microbial community structures of three different locations in the Oslofjord tunnel were assessed. Chemical micro-environmental conditions within the biofilm as well as water and biofilm chemical compositions were also presented.
- **Paper III**: In this study, the structure of the microbial community over time, at three locations in the Oslofjord tunnel was assessed. Analysis of biominerals, water chemistry, sources of nutrition, concrete deterioration over time was also performed. Metagenomics analysis was performed on selected biofilm samples to assess the metabolic potential of the microorganisms in the biofilms.

- **Paper IV**: In this study, biofilm formation and microbial succession on four different concrete surfaces, smooth and rough surface with absence or presence of steel fibers, exposed to the seawater in controlled laboratory environment, was investigated.

1.2 Scientific approach and limitations

Biodegradation of concrete is caused by a combination of biotic and abiotic factors. Biofilm communities are usually composed of a complex consortia of microorganisms with intricate interactions with the abiotic environment (Javaherdashti, 2017). Most of the studies of microbiologically induced deterioration (MID) has relied on bacterial cultivation techniques for detection and isolation of MID-related microorganisms and has resulted in simplified models to reduce the complexity inherent in multi-species biofilms (Dang et al., 2011). Standard microbial cultivation technique can only detect a small fraction of the microorganisms present (0.1-10%) (Theron & Cloete, 2000). Therefore, isolation of microorganisms from particular environments is not sufficient to be able to relate these microorganism to the biodegradation problem and has often failed to produce effective strategies for biocorrosion and biodegradation control (Machuca Suarez, 2019).

Deterioration mechanisms and microbial processes involved in MID of sewer systems are well-known and widely studied using cultivation techniques and simplified models (Wu et al., 2020), whilst knowledge about biodeterioration mechanisms related to subsea tunnels with reinforced sprayed concrete is limited. Degradation mechanisms involved in MID on reinforced concrete structures in marine environments are complex, and in-depth knowledge about MID in seawater is lacking. Difficulties to isolate specific microorganisms from the biofilm in order to analyse their effect on concrete biodegradation and separating various biotic and abiotic processes involved in MID are the main reasons for limited knowledge in this field.

Modern molecular microbiological methods are recognised as essential identification tools to overcome the limitations of cultivation techniques. In particular, next generation sequencing (NGS) of conservative V4 region of 16S rRNA gene, provides insight into biofilm communities from complex environments including identification of uncultured microorganisms which have not been studied before. Amplicon sequencing is a cost-effective method to investigate taxonomic composition of microbial communities of many samples which enables large scale projects. In this thesis, microbial identification, diversity, localization and successional patterns on sprayed concrete was investigated by NGS. Nevertheless, novel techniques come with limitations and challenges such as detection of numerous unknown species which increases the complexity of the problem even further. These microorganisms can directly be involved in MID or indirectly by interaction between different microbial populations in the biofilm (Machuca Suarez, 2019). Since NGS of 16S rRNA provide limited information about microbial diversity and identification of biofilm communities, shotgun metagenomics was used to assess microbial composition and potential metabolic profiles of biofilm samples from the Oslofjord subsea tunnel (**Paper III**). Reconstructed metagenome-assembled genomes (MAGs) in combination with NGS provide us with a more powerful methodology that gives better understanding of the complex MID mechanisms and microbial community involved in such processes.

The thesis presents two different and connected projects that I have carried out during the five years of my doctoral studies; 1) experiments on site in the Oslofjord subsea road tunnel (**Paper I-III**); and (2) a mesocosm study at defined conditions at the laboratory (**Paper IV**). **Paper I-III** describe the assessment of the composition, diversity, stratification and metabolic potential of the biofilm microbial communities in association with the sprayed concrete degradation and steel fiber corrosion. Biofilm composition and water chemistry were analysed at regular intervals during five years. The experimental work in the Oslofjord subsea tunnel was allowed to be performed only on specific dates planned for tunnel maintenance and our work in the tunnel could only be performed at night. All samples had to be kept frozen in dry ice during the 290 km drive to the laboratory. Preparation of samples for the microbial analysis and chemical analysis were performed at the Environmental Chemistry Laboratory at Chalmers. The DNA extraction and PCR amplification of the biofilm samples proved difficult, probably due to high metal concentrations, and different protocols for extraction had to be tested prior to collection of samples.

In parallel to the Oslofjord subsea tunnel study, a controlled mesocosm experiment was performed during 65 weeks in the laboratory where different types of concrete samples were exposed to seawater. We investigated how microorganisms colonize concrete surfaces over time in marine environment and how concrete surface and presence of steel fibers affect microbial community structure in the biofilm (**Paper IV**).

2 Introduction

In natural habitats and man-made systems, microorganisms, including bacteria, archaea, algae and fungi, colonize and grow on abiotic and biotic surfaces forming complex structures-biofilms (Flemming & Wingender, 2010). Biofilms consist of heterogeneous microbial cells embedded in a matrix of extracellular polymeric substances (EPS) which make up a three-dimensional scaffolding consisting mainly of polysaccharides, proteins, lipids and extracellular DNA (Flemming & Wingender, 2010). The EPS produced by microorganisms promote microbial adhesion to surfaces, keep the cells close together and enable cell-cell communication. The composition and structure of EPS depend on the type of biofilm cells, surrounding environment, local shear stress and availability of nutrients (Flemming et al., 2016). However, this is a simple description of biofilms as they are highly organised and dynamic structures that provide survival advantages for microorganisms such as easy access to nutrients, protection from hydration, facilitated gene transfer and promote resistance to extreme environments and aggressive compounds. Therefore, microbial biofilms are able to grow on most types of surfaces under large ranges of temperature, pressure, pH, salinity, UV radiation and nutrient conditions (Donlan, 2002; Flemming & Wingender, 2010; Stoodley et al., 1999).

The initial bacterial attachment to the surface depends on the physical and chemical surface characteristics. Nutrient presence provides a trigger for microbial communication ("quorum sensing") leading to microbial colonisation, adhesion and biofilm formation (Busscher & van Der Mei, 1995). Early colonizers determinate the structure and function of more mature biofilms (Dang & Lovell, 2016). In mature biofilms, the cells are embedded in EPS and separated by water channels which act as a crude transport system for the movement of nutrients and waste products. Mature biofilms are multi-layered structures and their response to the local environment is the result of community interactions that cannot be predicted by studying planktonic or single-species biofilms (Okabe et al., 2007; Stoodley et al., 1999).

Microbial colonization of man-made surfaces and their activities can have detrimental effects such as transmission of harmful microorganisms causing diseases, biofouling, biocorrosion, and damage to infrastructure. Ultimately undesired microbial activates may cause material changes with time (Little & Lee, 2007; Little et al., 2008) This phenomenon is known as biodeterioration or microbiologically induced deterioration (MID). MID involves the interaction of chemical, environmental, and biological factors which makes diagnosis of the degradation by biotic factors extremely difficult (Cwalina, 2008; Trejo et al., 2008).

2.1 Microbial induced concrete degradation

Biodeterioration of concrete is here termed MID whereas it is referred to as microbially induced concrete deterioration (MICD) or microbially induced concrete corrosion (MICC) in many research publications (Bertron, 2014; Gutierrez-Padilla et al., 2007; Márquez et al., 2013; Sanchez-Silva & Rosowsky, 2008; Wei et al., 2013). MID has mostly been observed in concrete structures exposed to aggressive environments such as sewer systems, drinking and wastewater systems, transportation in industries, marine structures, landfill leachate structures, acid mine drainage and offshore placements (Cwalina, 2014; Machuca Suarez, 2019; Wei et al., 2013). MID involves complex interactions driven by specific environmental conditions, substratum composition and nutrient availability (Harbulakova et al., 2013; Hudon et al., 2011; Monteny et al., 2001; Peyre-Lavigne et al., 2016). Microbial biofilms cause corrosion of concrete by

producing biogenic acids and minerals that dissolve or decompose the concrete matrix, which is a societal challenge with huge economic impact (Gaylarde et al., 2003; Wei et al., 2010). It has been estimated that repair and maintenance of biodeteriorated concrete cost billions of dollars per year in infrastructure and is often underestimated due to the fact that ongoing microbial interactions accelerate processes that would occur also in their absence (Gaylarde et al., 2003; Grengg et al., 2015; Roberts et al., 2002; Sanchez-Silva & Rosowsky, 2008). MID is considered to significantly reduce the lifetime of concrete structures from expected 100 years down to 30-50 (Wu et al., 2020). Microbial activity on concrete structures changes structural and functional properties of concrete, increases the concrete porosity, accelerates cracking, spalling, pitting and leaching of concrete matrix compounds (Harbulakova et al., 2013; Márquez et al., 2013). Additionally, by-products of MID such as hydrogen sulfide (H_2S) and ammonia (NH_3) are toxic even at low concentrations and can cause significant health related problems (Grengg et al., 2015).

Concrete is a heterogenous material, typically consisting of cement, water, aggregates (stone material and sand) and additional mixtures (optional) (Figure 1). Portland cement is the basic ingredient of concrete mixture consisting of Dicalcium Silicate ($2CaO \cdot Si_2$), Tricalcium Silicate ($3CaO \cdot Si_2$), Tricalcium Aluminate ($3CaO \cdot Al_2O_2$), Tetracalcium Aluminoferrite ($4CaO \cdot Al_2O_3Fe_2O_3$), Calcium Sulfate or Gypsum ($CaSO_4 \cdot 2H_2O$) and other minerals (Mehta & Monteiro, 2014)

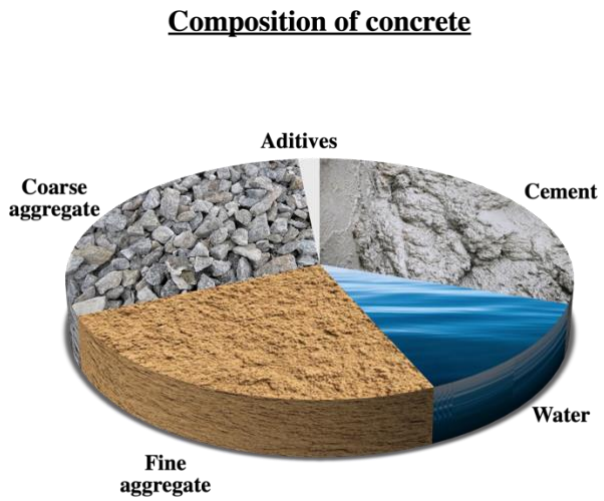

Figure 1. Diagram of standard concrete composition

Due to excellent compressive strength and lower tensile strength, concrete is the most applied construction material all around the world. To improve ductility and increase tensile strength, traditional cement concrete is reinforced with fibers or/and rebars (Simões et al., 2017). The fibers are bonded to the concrete mix and they are acting as a single structural elements (Figure 2). Fibers used in reinforced concrete include steel, glass, synthetic, and natural fibers. Steel fibers are one of the most commonly used fibers for reinforcement (Behbahani et al., 2011). Since steel fiber reinforcement reduces the possibility of concrete cracking or water permeating the concrete, it is commonly applied in tunnel construction, slabs and airport pavements (Berrocal et al., 2013; Berrocal et al., 2016).

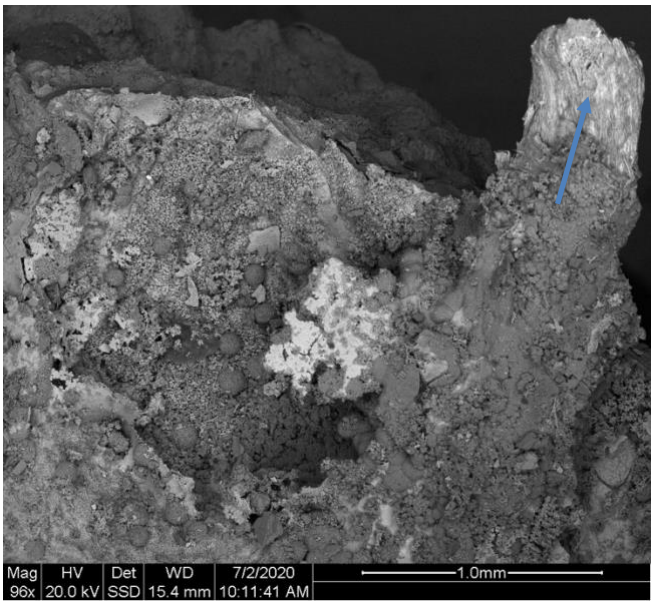

Figure 2. SEM images of steel fiber reinforced sprayed concrete.

In aggressive environments, various physical, chemical and biological factors can contribute to degradation of the cement paste matrix resulting in material deterioration and loss of strength. Concrete surfaces provide favourable conditions for microbial colonization due to suitable pH and high roughness with pores and cracks generated by the erosive action of water (Gaylarde et al., 2003; Hughes et al., 2013; Miller et al., 2012; Percival et al., 1999; Wei et al., 2013). Environmental conditions such as availability of nutrients, high relative humidity, certain temperature, high carbon dioxide concentration, high chlorine ion concentration and low pH facilitates biofilm formation on concrete surfaces (Noeiaghaei et al., 2017; Hughes et al., 2013). Microorganisms penetrate inside the concrete matrix through microcracks or capillaries that increases concrete porosity and permeability and facilitates chloride ingress leading to concrete deterioration (Little et al., 2008; Torres-Luque et al., 2014; Wei et al., 2010). Concrete pH is a critical parameter in determining bioreceptivity (Hughes, 2014). After construction, fresh concrete has pH in range of 11-13 as a result of hydration of Portland cement. The reaction with carbon dioxide can drop concrete pH to range 9–10 and leads subsequently to corrosion of steel fibers (Cwalina, 2008). Microorganisms have not been associated with this initial stage of MID (Gutierrez-Padilla et al., 2007; Permeh et al., 2019). Microbial colonization occurs once the pH of the concrete surface has dropped to around 9 (Noeiaghaei et al., 2017; Satoh et al., 2009). Microbial activities and succession on concrete can further reduce pH to less than 4 due to significant release of biogenic mineral acids such as sulfuric acid, carbonic acid, nitric acid and biogenic organic acids (acetic, lactic and butyric acids) (Alexander et al., 2013; Bertron, 2014; Peyre-Lavigne et al., 2015). Deterioration of concrete cannot be explain only by the effect of biogenic acids due to the many simultaneously ongoing microbial interactions within biofilms (Magniont et al., 2011).

2.2 Biodeterioration of concrete in sewer environment

Biodeterioration of concrete in sewer system is the most widely studied type of deterioration and general mechanisms of MID in sewer environments are well known (Dyer, 2017; Hughes et al., 2014; Noeiaghaei et al., 2017). In aquatic environments where sulfate ions are widely distributed, biogenic hydrogen sulfide (H_2S) is produced by sulfate reducing bacteria (SRB) under anaerobic condition in the bottom layer of sewer pipes (Wei et al., 2013). The presence

of hydrogen sulfide is usually the reason for further corrosion of concrete in sewer systems (Satoh et al., 2009). Once the pH of the concrete surface has dropped to ~ 9, and with sufficient nutrients available, moisture and oxygen, some species of sulfur-oxidizing bacteria (SOB) can attached to the concrete surface and oxidize hydrogen sulfide. Hydrogen sulfide can be oxidized into sulfur components with various oxidation states such as elemental sulfur (S^0) and thiosulfate (S_2O_3) (Wu et al., 2020). The neutrophilic SOB (NSOB) including *Thiobacillus thioparus*, *T. neapolitanus*, and *T. novellus* have a range of growth between 9 and 5 (Gutierrez-Padilla et al., 2007; Peyre-Lavigne et al., 2016) (Figure 3). The NSOB are replaced by acidophilic sulfur-oxidizing bacteria (ASOB) such as *Acidithiobacillus thiooxidans* and *Thiobacillus intermedius* when pH of concrete surface drops to around 4 (Hvitved-Jacobsen et al., 2002). ASOB can survive at very low pH such as 0.5 (Islander et al., 1991; Nica et al., 2000; Noeiaghaei et al., 2017). This microbial succession leads to accelerated concrete deterioration due to the ability of ASOB to create a highly acidic local environment by production of sulfuric acid. Sulfuric acid reacts with calcium hydroxide present in the concrete and causes concrete degradation due to formation of gypsum, ettringite and sometimes also the thaumasite (Peyre-Lavigne et al., 2016; Soleimani et al., 2013; Zhang et al., 2008).

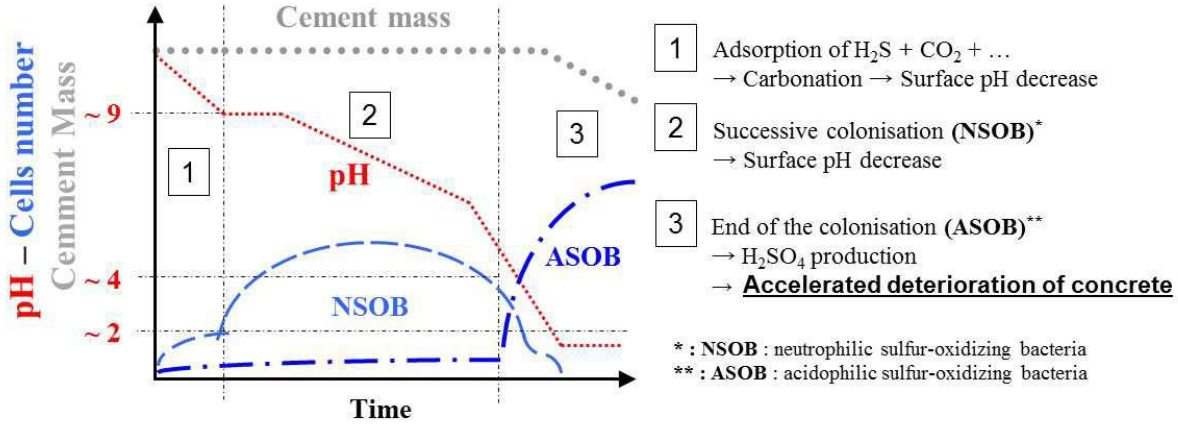

Figure 3. Adopted from (Peyre-Lavigne et al., 2016): Illustration of the microbial succession of sulfur-oxidizing bacteria (NSOB and ASOB) at the concrete surface of exposed cementitious materials.

Besides SOB, nitrifying bacteria are considered important for the degradation of concrete. Nitrogen converting bacteria are responsible for the oxidation of ammonia via nitrous acid and nitric acid (Cwalina, 2008; Sand & Bock, 1991). Nitrous acid (1) is produced by ammonia oxidizing bacteria (AOB) and ammonia oxidizing archaea (AOA) and nitrite-oxidizing bacteria (NOB) convert nitrous to nitric acid (2) (Table 1). The action of these acids on concrete promotes the formation of water-soluble calcium nitrate (3) and causes severe corrosion of the building materials (Ferrari et al., 2015; Gaylarde & Morton, 2003) (Table 1). However, biodeterioration of concrete caused by attack of nitrifying bacteria is less than biodeterioration caused by SOB, since this type of bacteria cannot grow at low pH (Soleimani et al., 2013).

Table 1. Biodeterioration of concrete caused by acid-producing microorganisms. (1) ammonia oxidizing bacteria and ammonia oxidizing archaea (AOB & AOA) oxidize ammonia to nitrous acid; and (2) nitrite oxidizing bacteria (NOB) convert nitrous to nitric acid; and (3) formation of calcium nitrate.

(1)	$2NH_4^+ + 3O_2 \rightarrow 2NO_2^- + 2H_2O + 4H^+$	*ammonia to nitrous acid*
(2)	$2NO_2^- + O_2 \rightarrow 2NO_3^-$	*nitrous acid to nitric acid*
(3)	$Ca(OH)_2 + 2HNO_3 \rightarrow Ca(NO_3)_2 + 2H_2O$	*calcium nitrate*

2.3 Biodeterioration of concrete in marine environment

In marine environments, mechanisms that govern microbial induced degradation of concrete seem to be more complex and quite different from those observed in freshwater environments. MID in marine environments is a complex phenomenon due to the fact that biological attack occurs in conjugation with abiotic processes such as carbonation, chlorine ingress and sulfate attack. These processes tend to increase the concrete permeability that reduces the strength of the structure and facilitates cracking (Mehta & Monteiro, 2014).

Fresh reinforced concrete structures have high pH values (around 12) that allow reinforcement to be protected by an oxide layer. When high concentrations of chloride ions ingress into the concrete matrix and come into contact with steel reinforcement, the protective cover may be reduced, leading to accelerated corrosion of the concrete reinforcement (Little et al., 2008; Torres-Luque et al., 2014; Wei et al., 2010). The main groups of microorganisms related to microbial induced corrosion (MIC) have been sulfate reducing bacteria (SRB), sulfur-oxidizing bacteria (SOB), iron-oxidizing/reducing bacteria (IOB or IRB), manganese oxidizing bacteria (MOB), and bacteria secreting organic acids and slime (Beech & Sunner, 2004; Ma et al., 2020). The role of these microorganisms can vary significantly depending on environmental conditions and parameters, such as temperature, pH, water flow and availability of nutrients, that support microbial proliferation on particular substratum.

Degradation mechanisms involved in MID of reinforced concrete in the marine environment are complex, and the knowledge about these mechanisms is relatively limited. The difficulty in separating various processes and groups of microorganisms involved in MID of reinforced concrete structures is the main reason for the lack of knowledge about the mechanisms involved.

2.4 Biodeterioration of sprayed concrete in subsea tunnels

Biodeterioration of sprayed concrete has been detected in several Norwegian subsea tunnels such as the Oslofjord, Freifjord and Flekkerøy tunnel resulting in cement paste matrix degradation and steel fiber corrosion in areas with leakages of saline groundwater (Hagelia, 2011a). Sprayed concrete reinforced with steel fibers is widely used in combination with rock bolts for rock support in Norwegian subsea tunnels. Concrete degradation and fiber corrosion in road subsea tunnels, due to abiotic and biotic attack, can result in destabilization of the rock mass, leading to potential safety risks, increased costs for maintenance and reduced overall lifetime of the tunnel. Degradation rates due to MID in subsea tunnels range from <0.5 to 10 mm/year, but in an extreme case more than 100 mm in less than five years has been observed. The sprayed reinforced concrete is designed for 100 years' service life, but detail investigations show that nowadays sprayed concrete lifetime in subsea tunnels is around 25 years (Hagelia, 2011b).

Since sprayed concrete has a very porous structure with high surface roughness, exposure to ion-rich water containing organic material, can facilitate microbial colonization on its surface. High ion concentrations in tunnel water are derived from dissolution of minerals within the rock mass and from saline groundwaters entering subsea tunnels. The presence of concrete cracks with water leakages in subsea tunnel environments further promotes microbial growth and biofilm accumulation on the outer surface of sprayed concrete.

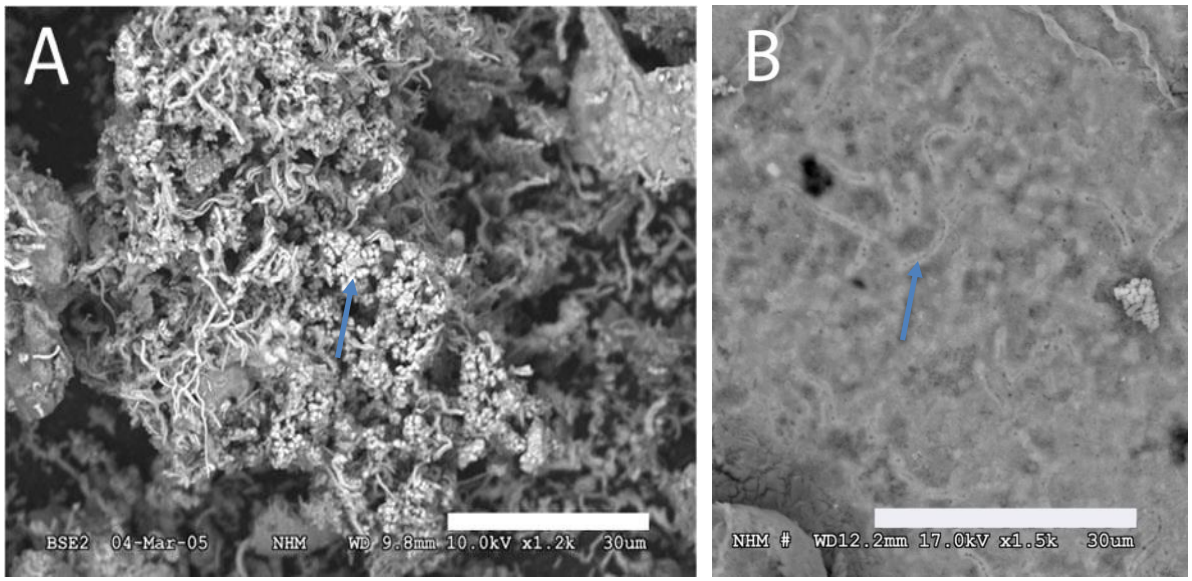

Figure 4. SEM images of biofilm (2005). A: Iron encrusted twisted stalks; and B: Sheet-forming microorganisms with internal disc-shaped cells and extracellular Mn-oxide deposits (Karačić et al., 2018).

The abiotic attack was found to mainly affect concrete adjacent to the rock mass and it was governed by infiltration of magnesium, sulfate and bicarbonate enriched saline ground water with pH ≈ 7.5-8 (Hagelia, 2011a). Abiotic degradation was characterised by calcium leaching, Mg-substitution for Ca in C-S-H, thaumasite, sulfate attack, decalcification and pop-corn calcite deposition. Biofilm accumulations was detected already after a few weeks after spraying operations in the Oslofjord subsea tunnel. Chemical reactions with iron-rich orange slime and manganese-rich dark/black soft to solid material were observed on concrete surfaces, caused by acidification of saline tunnel water (pH ≈ 7.5-8) and drop in pH down to 5.5-6.5. The studies performed by Per Hagelia between 2004-2011, showed that microbial biofilms, with iron- and manganese-oxidizing bacteria were involved in the degradation processes of the Oslofjord subsea tunnel concrete, but microbial identification was based on morphology only. Scanning electron microscopy (SEM) indicated two microorganisms, being Fe-rich or Mn-rich (Hagelia, 2007; Hagelia, 2011a, 2011b). Microorganisms with variably iron-encrusted twisted stalks were similar to *Gallionella ferruginea* or *Mariprofundus* sp. (Figure 4A) (Emerson & Moyer, 2002) and sheet-forming microorganisms with internal disc-shaped cells and extracellular Mn-oxide deposits similar to possible *Leptothrix discophora* (Emerson & Ghiorse, 1992) (Karačić et al., 2018) (Figure 4B).

The outer affected concrete material below the biofilms was rich in the biominerals Na-buserite, todorokite and ferrihydrite, along with Mg-calcite, calcite, aragonite, gypsum, thaumasite and brucite (Hagelia, 2007, 2011a). A multi-proxy study, involving SEM, concrete petrography, X-ray diffraction, microchemical analysis, and stable sulfur isotopes, demonstrated that:

a) acidification and calcium leaching were caused by biomineralisation and redox reactions within the biofilm
b) abiotic degradations involved thaumasite sulfate attack, magnesium attack, popcorn calcite deposition and chloride attack due to infiltration of saline ground waters.

The acidification processes were complex and presumably caused by oxidation of Fe(II) and Mn(II), redox reaction between dissolved Fe and Mn compounds, sulfuric acid formed by oxidation from temporarily formed sulfides within biofilms and formation of organic acids (Hagelia, 2007, 2011a; Hagelia, et al., 2020).

In a previous study in the Oslofjord tunnel, microbial community analysis using sequencing 16S rRNA gene was performed in 2011 by Thomas H.A. Haverkamp at the Centre for Ecological and Evolutionary Synthesis (CEES), the Department of Biosciences, University of Oslo, Norway. However, the dataset was small due to the use of Sanger sequencing of clone libraries that only enabled 61 sequences to be analysed. It was found that the biofilm microbial community at one specific tunnel locality was dominated by *Marinicella* sp., and a few chemolithotrophic bacteria; ammonia-oxidisers within *Nitrosomonas* and nitrite-oxidisers within *Nitrospinaceae*. However, no known sulfur converters or iron- and manganese-oxidizing bacteria were detected in this dataset (Karačić et al., 2018). The results of this pre-study clearly showed that biofilm communities involved in subsea concrete biodegradation are much more complex than initially anticipated. In order to understand and prevent biodegradation of concrete in subsea tunnels, further investigation of biofilm microbial diversity and metabolic activity is needed.

3 Materials and Methods

3.1 Site description - Oslofjord subsea tunnel

The Oslofjord subsea tunnel is located near Drøbak in Norway (59°39′53″N 10°36′47″E / 59.66472°N 10.61306°E) (Figure 5). The 7,306 m long tunnel has a width of 11.5 m and a maximum depth below the sea level of 134 m (Figure 6). The tunnel was opened in 2000. Few weeks after construction and spraying of the reinforced concrete, biofilms started to appear (Hagelia, 2007, 2011a) (Figure 7).

Figure 5. Geographical location of the Oslofjord subsea tunnel

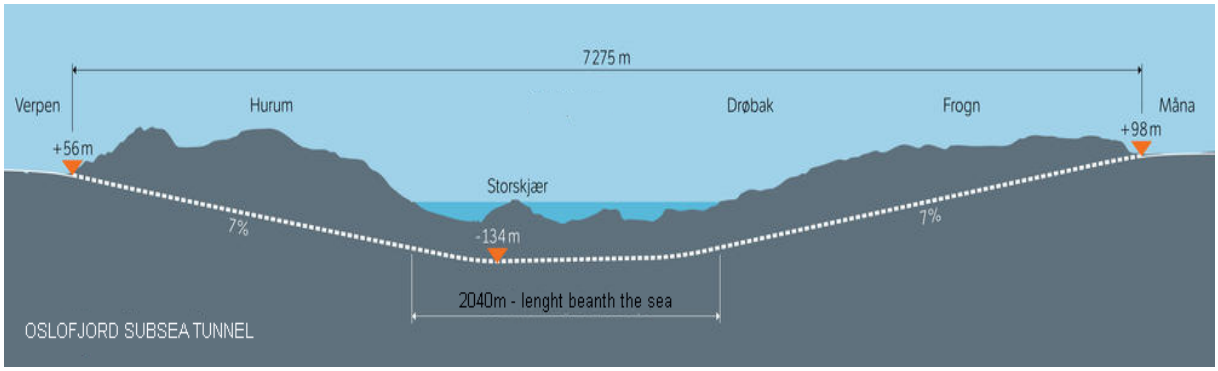

Figure 6. Overview of the Oslofjord tunnel showing the total tunnel length and depth/height relative to the sea level.

Figure 7. The Oslofjord tunnel entrance (left) and microbial biofilm material on sprayed concrete on the tunnel wall (right).

Biofilm samples were collected from the three different tunnel localities called: the *Main tunnel* (M), *Test site* (T) and *Pump station* (P) (Figure 8). These localities have been investigated at regular intervals since their establishment.

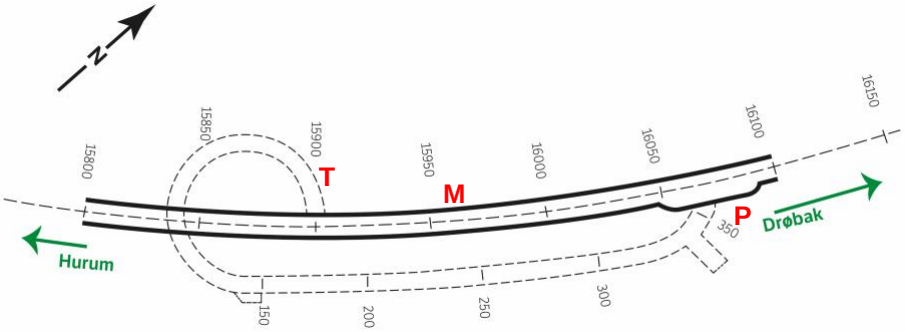

Figure 8. Schematic map of the tunnel site positions: the Test site (T), the Main tunnel (M) and the Pump station (P). Numbers refer to distances in meters.

The *Main tunnel* and the *Pump station* localities represent original concrete sprayed during tunnel construction in 1999 as permanent rock support. Sprayed concretes at these localities were based on a rapid setting cement (CEM I) and made with steel fibre and 5 % silica fume (by cement weight), using Al-sulfate as setting accelerator. The binder content (i.e. cement and silica fume) was 514 eq. kg/m^3 with water/binder (w/b)-ratio equal to 0.42. The concrete mix represents strength class B45 and durability class M45. The Oslofjord *Test site* was established by the Norwegian Public Roads Administration in March 2010 at a location where well-developed deterioration caused by microbial biofilm formation was observed on a 10-year old steel fiber reinforced sprayed concrete. In order to understand the effect of fiber type on concrete biodegradation, three subsites (T1-T3) were established with steel fiber and/or polypropylene fiber. The concretes at the *Test site* were based on CEM II/AV 42,5R and made with steel fiber (SF) and polypropylene fiber.

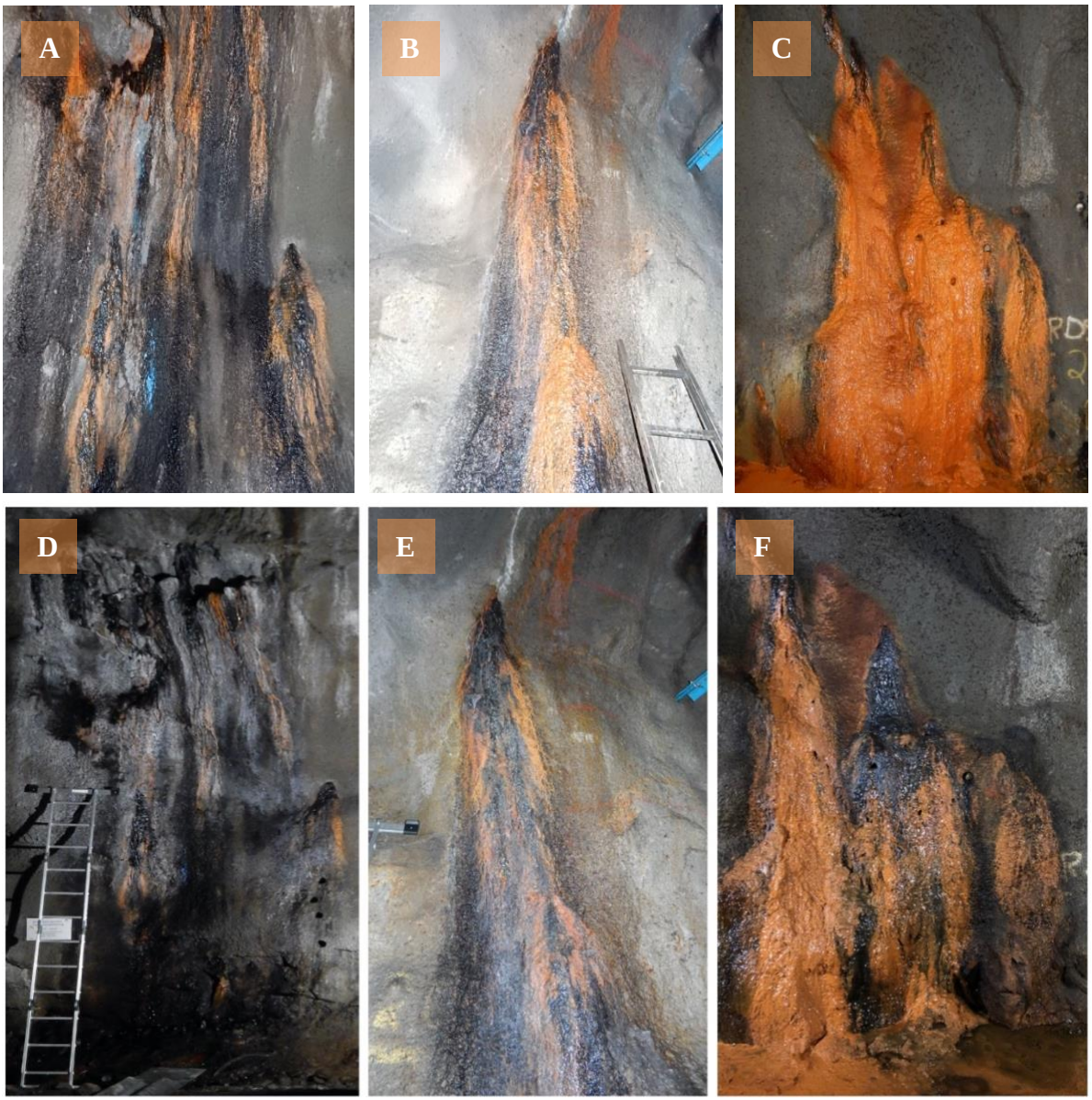

Figure 9. The biofilm appearance at the different sites of sampling performed in September 2015 (A-C) and September 2020 (D-F). From left to right: Test site; Main tunnel; and Pump station.

Concrete mixture at the Test subsites T1 and T2 were made with w/b = 0.43 (M45) and SF = 4 %, whilst the mixture at T3 subsite was made with w/b = 0.39 and SF = 10 %. Al-sulfate was used as setting accelerator. After new spraying operation in 2010, concrete thickness was increased ranging from 5-20cm. Soon after establishment of the new concrete at the Test site in 2010, biofilms were detected, suggesting that microbial colonization takes place at a very early stage (Hagelia, 2011a; Wilén et al., 2014). The bedrock is predominantly granitic gneiss and some pegmatite with joints and fault zones carrying clay minerals. The water temperature was close to 13^{o}C at the Pump station and 8-9 ^{o}C at the Main tunnel and Test site locations all year around. Light conditions varied from mostly very faint light to episodes with strong light once in a while during maintenance. Water flow was characterised by slow water seeping at all locations. Water from a large part of the tunnel Test site was fed to a local ditch - Ditch A. In 2013, rock coring at the Pump station location had caused new leakage points which led to new formations of yellowish-brown biofilms. Figure 9 shows changes in biofilm appearance in period of 2015-2020 at the three observed localities.

3.2 Mesocosms experiment

In order to understand the effect of concrete type and surface structure on microbial colonization and growth, a mesocosm experiment was set-up in the Environmental Chemistry Laboratory, Chalmers University of Technology and operated for 455 days (65 weeks). The mesocosm (Figure 10) was composed of 72 concrete samples divided in four separate recirculating systems: 1) smooth concrete surface without steel fiber reinforcement 2) smooth concrete surface with steel fiber reinforcement 3) rough concrete surface without steel fiber reinforcement 4) rough concrete surface with steel fiber reinforcement. Each system was containing: 1) an upper vessel with a drainage port 10.5 cm from the bottom to maintain a constant volume of water in the vessel (14 L), 2) a middle vessel (17.5 L) with a bottom drainage pipe, 3) a bottom container of 25 L. The water was recirculated from the bottom container to the upper vessel at 9 L/h by a peristaltic pump. Tube regulators at each upper vessel were controlled flow at 2mL/min. The mesocosm set-up was placed in a dark room and located in a fridge kept at 13ºC. More technical details about mesocosms set-up are explained in method section of **Paper IV**.

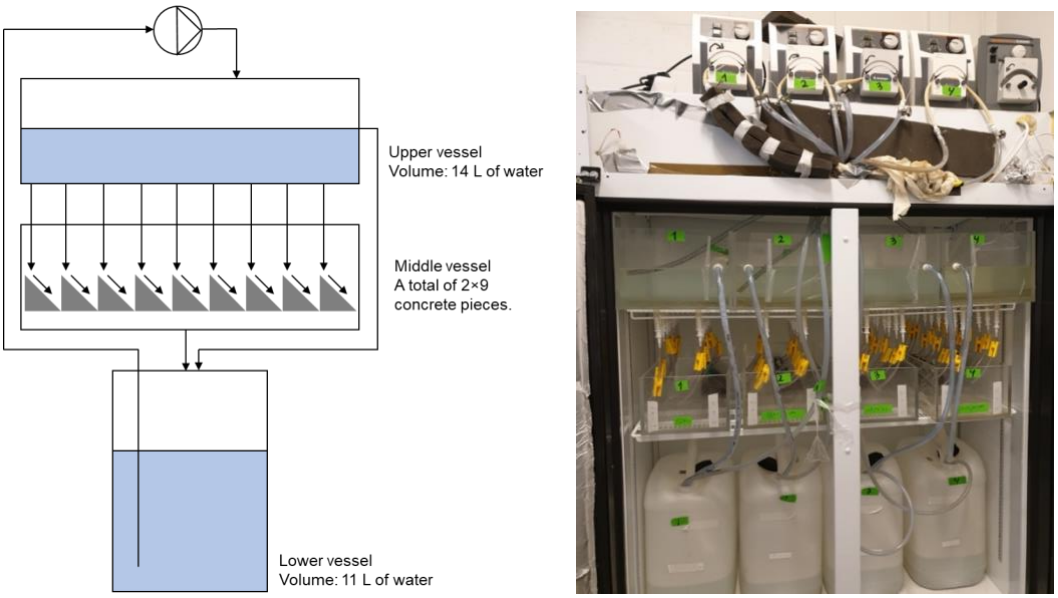

Figure 10. Overview of the mesocosms showing one of four parallel lines/systems (A); and photo of the experimental set-up (B).

Seawater used in the mesocosms experiment was collected at the Kristineberg Marine Research Station (University of Gothenburg) in Fiskebäckskil, Sweden. During collection, the seawater from 70 m depth was filtered through a 50 µm filter for debris removal. The water in the mesocosm was regularly replaced with new sea water, approximately every 3 weeks. The concrete samples were made with 5% microsilica ELKEM grade 920 added to RAPID Aalborg cement. Sand of D_{max}=0.4 mm was used for a water/binder ratio of 0.80. One batch of 20L concrete mix was prepared with addition of steel fibers, GSF 0520 (0.8kg), and another batch without steel fibers. The concretes were cast in 10×10×10 cm standard wooden moulds (EN 12390-1). After demoulding, the concrete blocks were cut diagonally into triangular prisms using a diamond blade. Thereafter, half of the samples were sand blasted to increase the surface roughness. All concrete pieces were stored in water for 30 days prior to starting the experiment.

3.3 Sampling

For studies presented in **Paper I-III**, biofilm sampling in the Oslofjord subsea tunnel was performed regularly during several years: 2015, 2016, 2017, 2019 and 2020. Friable biofilm material, ~10–15 mm thick, was gently sampled using metallic cores, whilst thin biofilms were harvested with a sterile scalpel (Figure 11). Sampling was aiming at obtaining a cross section of the biofilms, including a bit of degraded concrete underneath (Figure 12). Immediately after sampling the samples were frozen in dry ice/ethanol and stored in dry ice during transportation to the laboratory where they were kept at -80°C until nucleic acid extraction. Biofilm sampling were performed at three tunnel localities (the Pump station, the Test site and the Main tunnel) at different spots (in the x-y dimension).

Figure 11 Sampling procedures to capture the biofilm material. From left to right: Sampling of thin biofilm with a scalpel; Core sampling of thick biofilm; and hole after core sampling showing the concrete beneath (arrow).

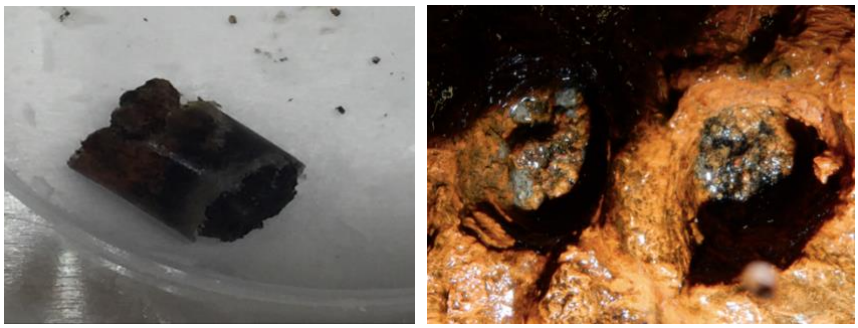

Figure 12. Frozen core of biofilm sample from the Oslofjord tunnel (A). Hole after core sampling showing depth of sampled biofilm material (B).

Biofilm material from each concrete sample (Figure 13) of the mesocosms set-up (**Paper IV**) were harvested using scalpel. Sampling was conducted after 21, 35, 43, 51 and 58 weeks of running the experiment and at each sampling occasion triplicate concrete pieces were taken out from the each mesocosm system. Biofilm material was scraped off from the concrete surface and collected in DNA-free tubes. Planktonic microorganisms in the water from the mesocosms systems and seawater were collected on 0.2 µm membrane filters (Sartorius Stedim Biotech, 47mm). Filters were stored at -20°C until DNA extraction was performed.

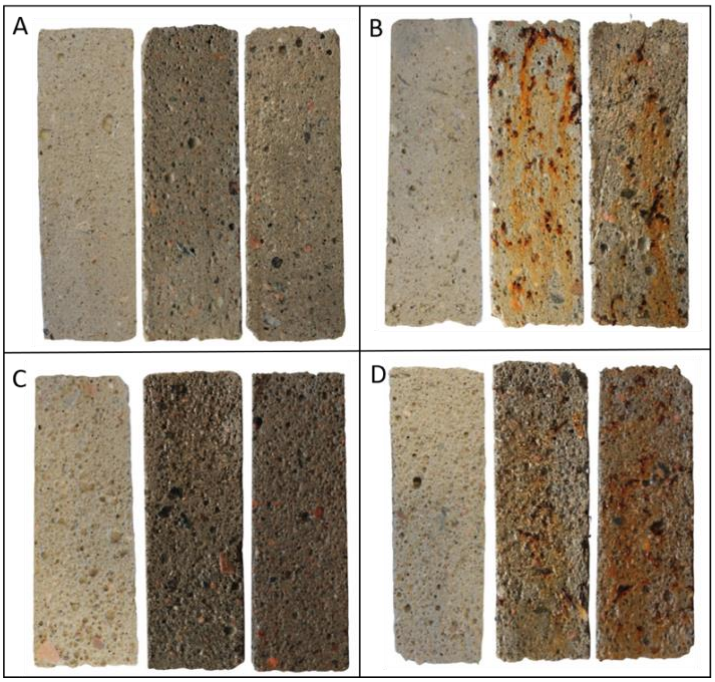

Figure 13. Concrete samples from the mesocosm. Day 1 (left), Day 301 (middle), Day 413 (right). (A) System 1, (B) System 2, (C) System 3, (D) System 4.

3.4 DNA extraction, PCR amplification and high throughput amplicon sequencing

Total genomic DNA was extracted using the Fast DNA spin kit for soil (MP Biomedicals) following the manufacturer's recommendations (**Paper I-IV**). In **Paper I**, a subset of the samples was split in half, where one half was extracted using Fast DNA spin kit for soil and the other half with the Zymo ZR-Duet DNA/RNA MiniPrep (Zymo Research). The concentration of the extracted DNA was measured using a Qubit 3.0 fluorometer (Thermo Fisher Scientific). The V4 hyper-variable region of the 16S rRNA gene was amplified in duplicates using the forward primer 515′F and the reverse primer 806R to cover both bacteria and archaea (Caporaso et al., 2011; Hugerth et al., 2014), with dual-index labelling (Kozich et al., 2013) with the following thermal cycle programming: activation at 98°C for 30 sec, denaturation at 98°C for 10 sec, annealing at 55.8°C for 30 sec, and extension at 72°C for 30 sec for 30 cycles, followed by final elongation at 72°C for 10 min. PCR reactions were conducted in 20µl reaction volume using Phusion Hot Start II DNA Polymerase (0.2µl) (Thermo Fisher Scientific), 5X Phusion HF Buffer (4µl), 10 mM dNTPs (0.4µl), DMSO (0.6µl), template DNA (1µl) and primers (10µM, 1µl each of forward and reverse primers). The duplicated PCR products were pooled and purified using the MagJet NGS Cleanup and Size Selection Kit (Thermo Fisher Scientific) and concentrations were measured by using the Qubit 3.0 and normalized at 6nM. The PCR products were pooled in equimolar amounts, the concentration and size were confirmed by TapeStation 2200 (Agilent Technologies) and sequencing was performed on an Illumina MiSeq using the MiSeq Reagent Kit v2 (**Papers I and II**) and MiSeq Reagent Kit v3 (**Papers III and IV**).

3.5 Bioinformatics and statistical analysis

Raw sequence reads were processed following two principally different approaches in this thesis. In **Paper I**, the reads were clustered into operational taxonomic units (OTUs) using the UPARSE workflow (Edgar, 2013), while in **Papers II-IV**, the more recent approach of amplicon sequence variants (ASVs) was used, with either UNOISE (Edgar, 2016; Edgar & Flyvbjerg, 2015) within USEARCH (**Paper II**) (Edgar, 2010), or a combination of DADA2 (Callahan et al., 2016) and VSEARCH (Rognes et al., 2016) (**Papers III** and **IV**). With the approach of OTUs, the reads within a specified similarity threshold (97%) are clustered together into the OTUs. Although this approach can be robust for grouping sequences, the centroid sequence, which represent the OTU, depends on the other sequences in the run and is therefore not comparable to OTUs generated from other samples in other runs (Modin et al., 2020). The approach of ASVs is based on denoising using algorithms to differentiate between true ASVs and erroneous sequences. The resulting ASVs therefore represent true biological entities that can be compared between samples from different studies. The ASV approach also has higher precision for detecting rare taxa (He et al., 2015; Modin et al., 2020). The OTUs or ASVs are collected in count tables. For the **Papers III** and **IV**, the resulting count tables from DADA2 and VSEARCH were combined in a consensus table of ASVs detected in both pipelines to minimize presence of low abundant and potentially erroneous ASVs (Modin et al., 2020). For classification of the OTUs or ASVs in the count tables, the Silva taxonomy was used, either within MIDAS v2.0 and 2.1 (McIlroy et al., 2015) in **Paper 1** and **II,** or Silva v132 (Quast et al., 2012) in **Paper III** and **IV**. Classification was carried out using the RDP classifier (Wang et al., 2007) in **Paper I**, and later on with Sintax (Edgar, 2016) in **Paper II-IV.** Detailed information on pipeline settings is available in the method section of each appended paper.

In **Papers I** and **II**, multivariate statistics, richness and evenness calculations; and data visualization were conducted within the R packages ampvis 1.14 (Albertsen et al., 2015), vegan (Oksanen J, 2017) and picante (Kembel et al., 2010). Beta diversity was estimated using pairwise Sørensen and Bray-Curtis dissimilarities and visualized using principal coordinate analysis (PCoA). Differences in beta diversity were tested for using permutational multivariate analysis of variance (PERMANOVA, adonis). The standardised effect size (SES) for pairwise Sørensen dissimilarities was estimated in vegan to test for random community assembly, with a null-model that preserves species richness and species incidence. Unweighted nearest taxon index was estimated using picante with the null-model "taxa.labels" at 999 iterations to test for phylogenetic clustering among closely related taxa (Webb et al., 2002). Differences in community richness and evenness was tested for using Welch's test followed by post-hoc analysis using the Games-Howell test.

In **Papers III and IV**, taxonomic Hill numbers were used to calculate alpha and beta diversity (Chao et al., 2014; Jost, 2006). The parameter q is the diversity order. At a q of 0, all ASVs are considered equally important, whilst at q=1 each ASV is weighted according to its relative abundance in a sample. Therefore, ${}^{0}D$ is equal to the number of ASVs found in a sample (richness) while ${}^{1}D$ can be interpreted as the number of "common" ASVs for α-diversity (Jost, 2007; Modin et al., 2020). In order to determine the dissimilarity caused by compositional turnover between samples and to assess the roles of deterministic and stochastic factors for microbial community assembly, the Raup-Crick null model (Chase et al., 2011; Raup & Crick, 1979) adapted for Hill-based dissimilarities (Modin et al., 2020) was used. Permanova (9999 permutations) was used to assess the statistical significance of differences between groups of samples (Anderson, 2001).

Data visualisation, calculation of alpha and beta diversity, null modelling, and permanova tests presented in **Papers III and IV** were conducted in qdiv. Univariate statistical tests were performed using the Real Statistics add-in to Excel. The DESeq2 method (Love et al., 2014) to tests differential abundance of ASVs with time and between systems was carried out in R (R Core Team, 2020). Details about the analysis are provided in the methodology section and supplementary of **Papers III and IV**.

Eight samples from the long-term study (2016-2020) in the Oslofjord tunnel were selected for shotgun metagenomics (**Paper IV**). Libraries were prepared with a TruSeq PCR-free kit (Illumina) and sequencing was performed on NovaSeq6000 with a 2x151 setup, yielding 268 million pair-reads. Detail information about further bioinformatic procedure metagenomics could be found in methods section in appended **Paper III**. The relative abundance of 401 constructed metagenome assembled genomes (MAGs) was estimated with coverM (*https://github.com/wwood/CoverM*). MAGs had >50% completeness and <10% contamination. Taxonomic classification was done with GTDB-Tk (Chaumeil et al., 2020) using the GTDB R06-RS202 reference (Parks et al., 2018; Parks et al., 2020). Protein coding sequences in all the MAGs were identified with Prodigal (Hyatt et al., 2010). HMM profiles from TIGRFAM and PFAM were used to identify key genes in the nitrogen and sulfur cycle with HMMER3 (Eddy, 2011). Genes linked to iron oxidation and iron reduction were identified with FeGenie (Garber et al., 2020).

3.6 Water and biofilm chemical analysis

In **Paper I**, water samples were analysed by different commercial laboratories according to their routines. In the field, pH was measured using either indicator strips (accurate to pH ± 0.1), or pH meter (accurate to pH ± 0.01) (**Paper I-III**). The water samples from the Oslofjord subsea tunnel were collected directly in 500 ml sterile bottles, from the dripping water with care taken to avoid contamination from the biofilms (in papers presented as WR- water from rock mass without contact with biofilms), and from dripping water with biofilm and concrete interaction (in papers presented as WCB – water in contact with biofilm). Bottles with water samples were stored in dry-ice during transportation to the laboratory and filtered through 0.45 µm filters before analysis (**Paper I-III**), whilst 0.2 µm filter was used for filtration of the water samples from the mesocosms systems and from the new seawater (**Paper IV**). Selected metals were quantified by quadrupole Inductivity Coupled Plasma-Mass Spectrometry (ICP-MS) using Thermo Fischer Scientific iCAP Qc. and dissolved ions were analysed using a Dionex ICS-900 ion chromatograph (**Paper II-IV**).

In **Paper II**, biofilm samples for chemical analyses were homogenized and dried at 105°C. Total solids (TS) and volatile solids (VS) of the biofilms were analysed according to Standard Methods 2490 A-D (APHA, 1998).

In **Paper IV**, total organic carbon (TOC), dissolved organic carbon (DOC) and total nitrogen were measured using a Shimadzu TOC analyser and alkalinity was measured (TitroLine X800) according to Standard methods (APHA, 1998). At regular intervals, pH and conductivity of water samples from the mesocosms systems and from the new seawater were measured by a WTW Multiliner 363IDS.

3.7 Microsensor measurements (Paper II)

In **Paper II**, in-situ profiles of pH and oxygen in the biofilms were measured at several occasions in 2017. Measurements were performed from the outer surface of the biofilm to the inner parts towards the concrete surface (Figure 14). The Clark-type oxygen microsensors (tip diameter 50 µm; OX-50, Unisense) were calibrated prior to measurements at the Pump station site with 100% oxygen saturated saline groundwater at a temperature of 13°C and 30% salinity in a calibration chamber (CAL300) following Unisense calibration protocol. The pH microsensor (tip diameter 50 µm, linear range pH 4-9; pH-50, Unisense) was used in combination with a reference electrode (tip diameter of 50 µm; REF-50, Unisense) and linearly calibrated in-situ with three pH buffer points (pH 4, 7 and 9). Microelectrodes were connected to an eight-channel Field microsensor multimeter (Unisense) and fixed in a motorized micromanipulator (MM33-2, MC-232; Unisense A/S) controlled by software (SensorTrace PRO; Unisense A/S). Before measurements, biofilm depth was estimated using a spent microsensor needle. The microsensor tip was positioned at the water/biofilm surface defined as the starting position (0 µm on graphs) and microprofiling was performed in steps of 500 µm with 10 seconds of waiting period before each measurement. Profiling measurements using microsensor at the Oslofjord Pump station location proved very difficult due to electrical disturbance and water leakage from the tunnel ceiling.

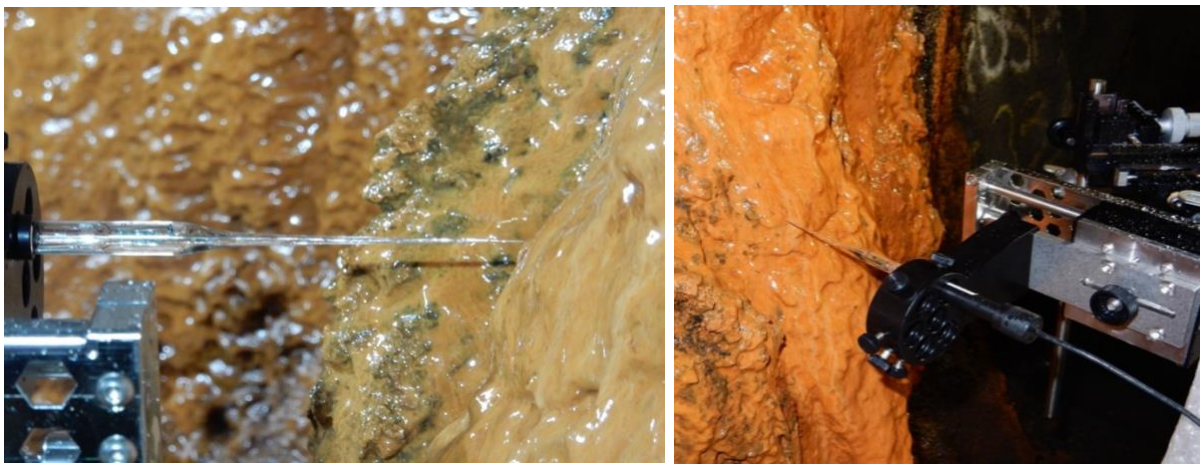

Figure 14. An oxygen microsensor with the tip positioned at the biofilm-water interface. Microsensors were used for measurements of profiles of pH and oxygen through the biofilm.

3.8 Analysis of concrete, biominerals and biota (Papers II-IV)

Scanning Electron Microscopy (SEM)

Uncoated handpicked samples and thin sections were mounted on carbon tape for analysis by SEM (**Paper II**). Chemical point analyses (1-2 μm^2) were performed on pristine untreated sample materials and a few thin sections, using a Hitachi 3600 N scanning electron microscope with an energy dispersive spectroscope (EDS) unit from Thermon Electronic Corporation. The instrument was operated with an accelerating voltage 15 kV at high vacuum. The vacuum chamber had an option for freezing, and bacterial wet samples were frozen to - 30^{o}C prior to analysis. In **Paper III**, selected domains of biofilm, concrete chips and thin sections were analysed by SEM using a Hitachi S–3600N. X-ray element maps and back scatter electron images were captured and followed by spot analyses (spot size 5 µm). For XRD, small samples

were ground in agate mortars under ethanol and left to dry before being mounted on sample holders and run in a Siemens D 5005 Spectrometer. Diffractograms were recorded from 2º to 60º with step size 0.05º on the 2-Theta scale for 58 minutes. The instrument was set to 40 kV and 40 nA using Ni-filtered CuKα radiation with wavelength λ=1.54 Å. The diffractograms were checked versus the Powder Diffraction Files database from the International Centre for Diffraction Data (PDF4+ 2020 database). In **Paper IV**, small pieces of selected concrete samples from the mesocosm were mounted on a metal stub for SEM. Pristine and uncoated samples were investigated under high-vacuum mode at an acceleration voltage of 20kV and working distance 10.2–14.3mm using a Quanta200 ESEM (FEI) The Oxford Inca Energy Dispersive X-ray (EDX) was used for chemical characterisation and chemical point analysis and INCA EDS software was used got data analysis. Other samples were analysed in a Hitachi S–3600N Scanning Electron Microscope (SEM) available at the GeoLAb, Natural History Museum, University of Oslo. The instrument is equipped with a Bruker XFlash® 5030 energy dispersive X-ray detector (EDX), running on Quantax 400 (Esprit 1.9), for semi-quantitative elemental analysis and hyperspectral mapping, with <127 eV FWHM at MnKα energy resolution. Samples were mounted on carbon tape and analysed in variable pressure (VP) mode (20 Pa), 15.0 kV accelerating voltage, ca 50nA beam current.

.

4 Results and Discussion

4.1 Does the DNA extraction method work? (Paper I)

In order to find a suitable method for DNA extraction of biofilms samples from the Oslofjord subsea tunnel concrete, two different bead-beating based methods were tested on three parallel samples. Previously, it has been shown that the choice of DNA extraction methods may have large impact on the microbial composition, even for methods using the same principles of bead-beating followed by separation of DNA (Vanysacker et al., 2010). The two DNA extraction kits produced similar results in microbial composition, as seen by the fact that the three biological samples separated well in the PCA (principal component analysis) ordination, with no apparent effect on the separation by the choice of DNA extraction methodology (Figure 15). However, to be consistent, the DNA extraction of biofilm samples, in preformed studies presented in appended **Papers I-IV**, was based on one method only, the FastDNA spin kit for soil.

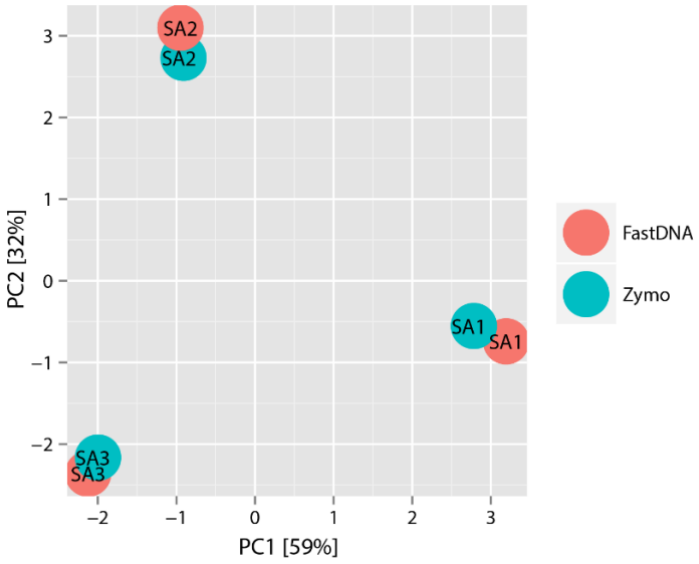

Figure 15. PCA ordination of microbial community data obtained by the two DNA extraction kits: FastDNA spin kit for soil (FastDNA) and Zymo ZR-Duet (Zymo).

4.2 What are the local environmental conditions?

4.2.1 Chemical characteristics of the water in the Oslofjord subsea tunnel (Papers I-III)

Water samples from the Oslofjord tunnel were taken from dripping water that had passed through rock mass without interaction with the concrete and biofilm and from the water after interaction with the concrete and biofilm. Generally, water samples of saline groundwater from the Oslofjord subsea tunnel had a composition quite similar to the seawater with high concentrations of chloride, sodium, sulfate and magnesium. Concentrations of calcium, magnesium and vanadium were higher in the water that had been in contact with biofilm and concrete, compared to the water that had only been in contact with the rock mass. The concentrations of iron, manganese and ammonium were in very low concentrations in all water samples taken either after contact with biofilm and concrete or only in contact just with the rock mass (Table 2).

Table 2. Chemical composition of the water samples taken either after contact with biofilm and concrete or only in contact with rock mass. *=Water interacted with Concrete and Biofilm (WCB), **=Water interacted only with Rock mass (**Paper II**).

		Pump station 2015		*Pump station 2016*		*Pump station 2016/2017*		*Test site 2016*		*Test site 2017*		*Main tunnel 2017*	
Sample type		**WCB***	**WR****	**WCB***	**WR****	**WCB***	**WR****	**WCB***	**WR****	**WCB***	**WR****	**WCB***	**WR****
Sample		SK1	SK2	SK3	SK4	SK5	SK6	SK7	SK8	SK9	SK10	SK12	SK11
Mg	mg/l	2232	1147	1323	1201	1150	821	1416	1400	1121	1224	1879	1291
Al	mg/l	0.35	0.67	0.31	0.37	0.32	0.35	0.64	0.38	0.53	0.39	0.78	0.55
Ca	mg/l	604	292	343	297	274	236	362	314	384	360	513	486
Ti	mg/l	0.96	0.84	1	0.88	0.81	0.78	0.99	0.89	0.62	0.67	0.83	0.82
V	mg/l	0.26	0.13	0.15	0.13	0.13	0.11	0.16	0.15	0.14	0.16	0.21	0.15
Cr	mg/l	0.01	0.00	0.01	0.21	0.00	0.00	0.01	0.01	0.01	0.01	0.01	0.01
Mn	mg/l	1.32	1.28	1.31	1.28	1.03	1.28	1.36	1.54	2.11	1.7	1	1.09
Fe	mg/l	0.01	0.01	0.01	0.01	0.01	0.01	0.02	0.02	0.17	0.17	0.01	0.02
Co	mg/l	0.003	0.002	0.002	0.004	0.001	0.005	0.003	0.002	0.002	0.003	0.003	0.003
Ni	mg/l	0.74	0.24	0.78	0.94	0.80	1.19	1.56	1.23	0.004	1.16	5.32	0.03
Cu	mg/l	0.42	0.26	0.33	0.39	0.29	0.46	0.49	0.47	0.23	0.46	0.23	0.88
Zn	mg/l	1.02	0.80	1.07	5.98	1.14	3.38	3.37	3.24	0.09	3.24	0.24	4.77
Cd	mg/l	0.001	0.002	0.001	0.002	0.001	0.002	0.002	0.002	0.006	0.004	0.002	0.009
Pb	mg/l	0.032	0.037	0.039	0.082	0.048	0.172	0.097	0.125	0.068	0.167	0.32	0.006
Cl	mg/l			20000	22400								
SO_4	mg/l			2700	3260								
NO_3	mg/l			3.2	< 0.5								
NH_4	mg/l			0.74	< 0.32								

4.2.2 Chemical characteristics of the water in the Mesocosms experiment (Paper IV)

The chemical composition of the water that had percolated over the concrete blocks in mesocosms systems 1-4 and seawater used in the mesocosms experiment is presented in Table 3. The water in systems 1-4 had significantly higher pH, alkalinity and conductivity compared to the seawater although the average values were in the same range.

Table 3. Characteristics of the concrete (presence/absence of steel fiber reinforcement and surface structure) and chemical composition of the water in systems 1-4 and in the sea water.

Parameter	**System 1**	**System 2**	**System 3**	**System 4**	**Seawater**
Reinforcement	no fiber	steel fiber	no fiber	steel fiber	-
Surface structure	smooth	smooth	rough	rough	-
pH	8.32±0.08	8.36±0.07	8.35±0.07	8.38±0.075	8.18±0.12
Conductivity (mS/cm)	52.93±1.70	52.81±1.36	53.22±1.30	53.89±1.65	50.41±1.07
Alkalinity ($mgHCO_3/l$)	126±14	130±4	123±7	135±9	102±15
DOC (mg/l)	4.32±2.21	5.23±3.27	4.84±2.80	4.27±2.87	2.65±1.38
N_{tot}(mg/l)	0.068±0.067	0.100±0.079	0.092±0.073	0.066±0.053	0.066±0.066
Ca (mg/l)	503±100	513±152	471±113	464±128	458±175
Si (mg/l)	2.361±1.310	2.187±1.074	2.212±1.257	2.137±1.207	1.909±1.027
Fe (mg/l)	0.214±0.023	0.216±0.015	0.202±0.023	0.216±0.026	0.217±0.024

Differences in pH values of water from the systems indicated that the iron fiber and surface structure had an impact. However, concentration of ions, metals, and dissolved organic carbon (DOC) were not significantly different between the water from mesocosms systems, indicating that the experiment had minor effect on these parameters.

4.2.3 Biofilm chemical characteristics (Paper II)

Concentrations of selected metals of several biofilm samples from the Oslofjord tunnel taken in period the 2015-2017 are shown in Table 4. Higher iron and calcium concentrations were detected in orange/dark rusty samples, whilst dark/black biofilm samples contained higher concentration of manganese. Very low concentration of Cu, Cr, Ti and Pb were detected in the both types of biofilms. The average volatile solids concentration of the selected biofilm samples was 12.6 ± 0.7% (average ± st.dev.). The positions of the biofilm samples are presented in the Supplementary material of **Paper II**.

Table 4. Biofilm chemical characteristics. Samples collected in 2015, 2016 and 2017.

		Pump station			*Test site*			*Main tunnel*		
Biofilm description		black	orange	orange	orange/mix	orange/mix	black	black	mix	black
Mg	mg/g	23.04	36.97	39.65	17.77	14.20	17.14	29.19	27.75	2.40
Al	mg/g	2.91	0.55	2.00	1.58	1.25	1.94	14.56	13.69	0.72
Ca	mg/g		30.94	38.20	22.10	20.84	23.24	17.85	50.47	6.99
Mn	mg/g	284	260	75	90	133	225	40	39	33
Fe	mg/g	157	538	792	209	246	103	23	18	17
Ti	mg/g	0.19	0.09	0.21	0.13	0.06	0.13	1.14	1.03	0.01
Cr	mg/g	0.00	0.00	0.00	0.01	0.00	0.00	0.03	0.03	0.00
Co	mg/g	0.01	0.03	0.00	0.02	0.01	0.01	0.02	0.02	0.00
Ni	mg/g	0.33	0.11	0.24	0.18	0.08	0.07	0.07	0.08	0.19
Cu	mg/g	0.09	0.07	0.25	0.16	0.15	0.04	0.14	0.15	0.08
Zn	mg/g	0.50	0.79	0.61	1.06	0.51	0.53	2.46	0.36	0.40
Pb	mg/g	0.05	0.04	0.09	0.07	0.07	0.04	0.04	0.04	0.03
TSS	g/L	240	219	220	280	363	350	166	131.8	93
Volatile fraction	%	11.7	13.80	12.8	12.76	13.56	12.0	11.87	12.59	12.3

4.2.4 Biofilm microgradients of pH and dissolved oxygen (Paper II)

The measured dissolved oxygen (DO) profiles at the Pump station site revealed a relatively stable aerobic microenvironment with differences among local spots with varying superficial water flow rate. Measured DO decreased from 9 mg/l at the biofilm-water interface to below 3 mg/l in the inner biofilm regions close to the concrete at approximately 10000 µm biofilm depth (Figure 16A). In biofilm with high water flow, the DO concentration profiles were steeper compared to lower flow. Results from pH microsensor profiling showed that pH slightly decreased from 8.2 to 7.78 from the biofilm-water interface towards the bottom of the biofilm (Figure 16B)

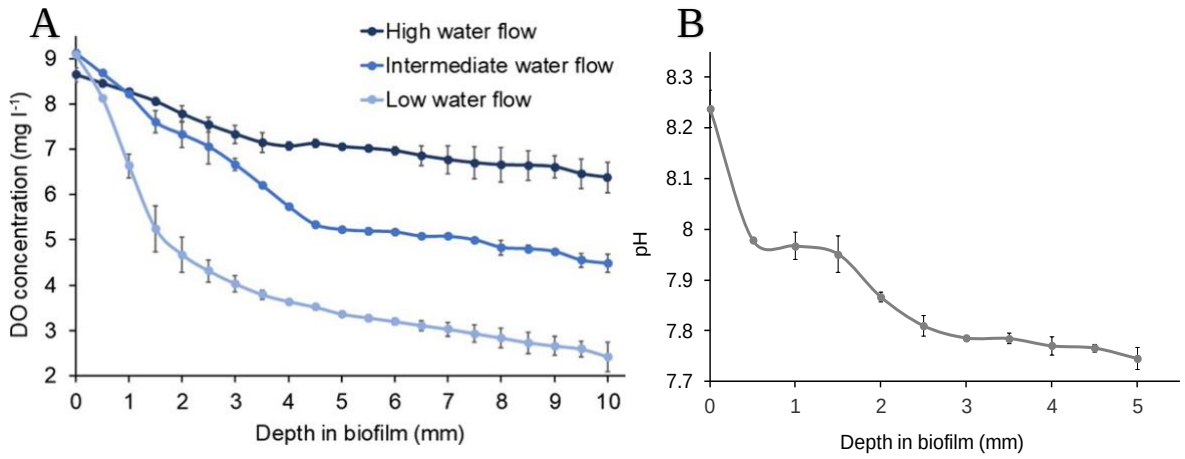

Figure 16. Profiles measured with microsensors; DO profiles across 1 cm thick biofilm exposed to different water flow rates (A); pH profile across 0.5 cm thick biofilm (B). For each data point, the mean value and standard deviation of 3 profiles is shown.

4.3 Who is there?

4.3.1 Microbial community composition in the Oslofjord subsea tunnel biofilms

Taxonomic analysis of the 16S rRNA gene sequences from biofilm samples from the Oslofjord subsea tunnel, taken in the period 2015-2020, revealed that the microbial communities from the three tunnel locations were composed both of *Bacteria* and *Archaea*. The major phyla detected at the Pump station, the Main tunnel and the Test site were *Proteobacteria*, *Planctomycetota*, *Crenarchaeota*, *Bacteroidota*, *Nitrospinota*, *Actinobacteriota*, *Cyanobacteriota*, *Nitrospirota*, *Verrucomicrobiota* and *Acidobacteriota* (**Paper I-III**) (Figure 17).

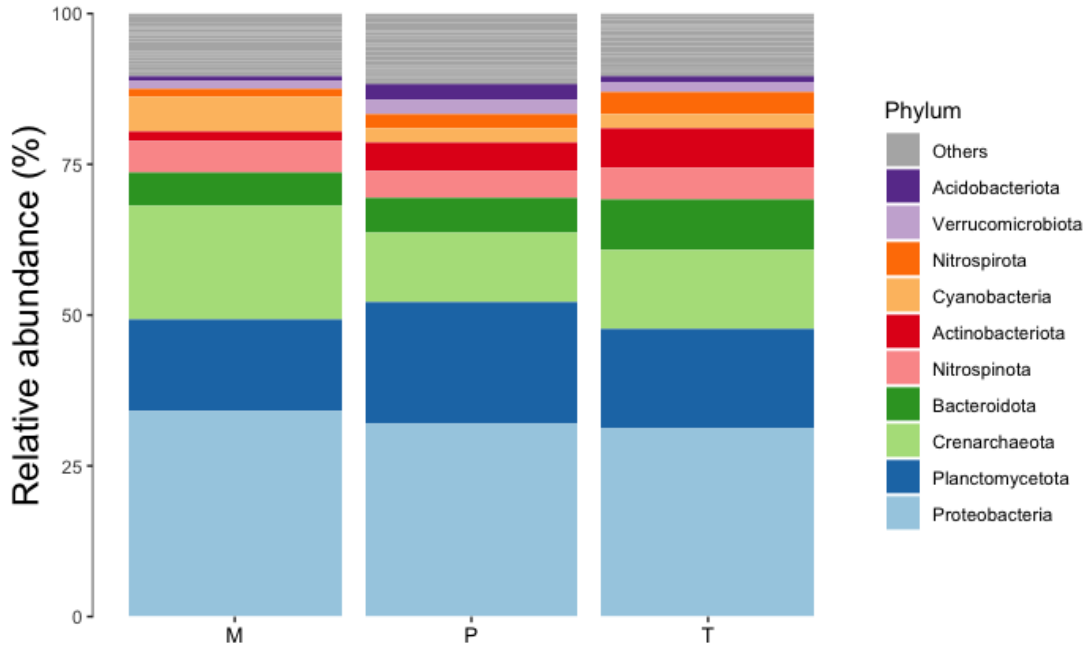

Figure 17. Relative abundance of phyla discovered in the biofilm communities at three tunnel locations (the **M**ain tunnel, the **P**ump station and the **T**est site)

The microbial community composition of the subsea tunnel biofilms was different from biofilms associated with concrete degradation in sewer pipes, where sulfur-oxidizing and -reducing clades are numerically and functionally important contributors (Gomez-Alvarez et al. 2012; Cayford et al. 2017). The subsea tunnel biofilm communities had similarities in composition to sediments in the Oslofjord (Håvelsrud et al. 2012), as well as other marine sediments and biofilms (Choi et al. 2016; McBeth and Emerson 2016), with high abundance of autotrophic nitrogen- and iron-oxidizing microorganisms and several taxa of marine heterotrophic bacteria.

The top 25 ASVs from the Oslofjord subsea tunnel sites are shown in Figure 18. At genus level, high abundance of autotrophic nitrogen converting microorganisms (*Nitrosomonas, Nitrosopumilus, Nitrospina, Nitrospira*) were observed at the three tunnel locations.

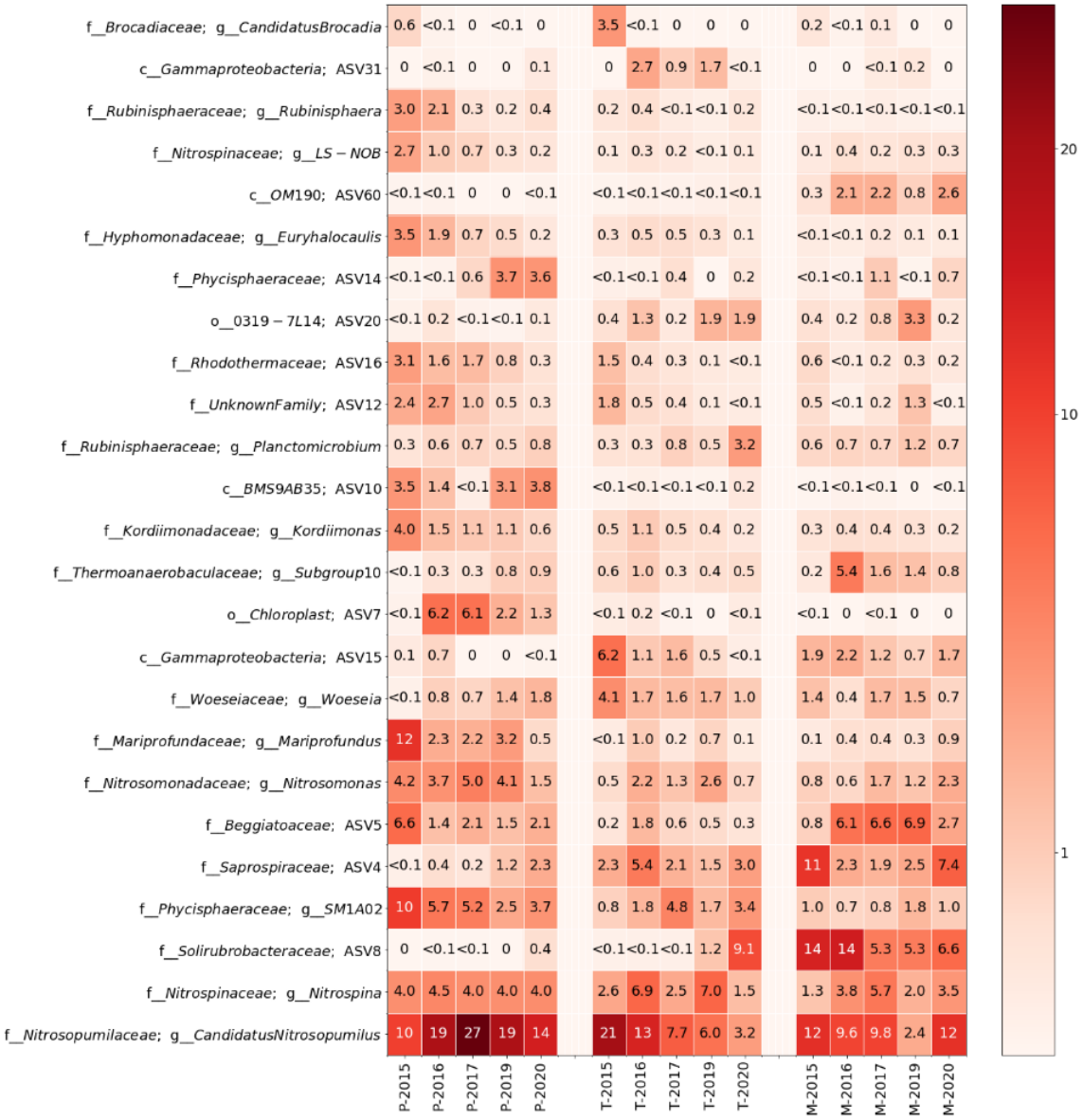

Figure 18. Heatmap showing the 25 most abundant SVs in the biofilm at the Pump station (P), Test site (T) and the Main tunnel (M). Abundance data showing average values of sampling at each sampling occasion (2015, 2016, 2017, 2019, 2020)

The archaeon *Nitrosopumilus sp.* was most abundant microorganisms detected in all biofilm samples. Ammonia-oxidizing archaea are ubiquitous in marine water and well-adapted to low substrate concentrations and low oxygen environments (Park et al., 2010). Nitrite-oxidizing bacteria (NOB) of genus *Nitrospina,* typically found in marine environments, was observed in high abundance in the Oslofjord subsea tunnel biofilms with several samples having >6% relative abundance. Genus *Nitrosomonas* sp. belonging to the anoxic marine sediment group of AOB (Urakawa et al., 2006) was present at an average relative abundance of 2.1%. Genus *Nitrospira* sp. capable of nitrite oxidation (NOB) and presumably also ammonia oxidation (AOB) (Daims et al., 2015), were detected in relative abundance of 1.2% in samples taken during the period of November 2015 and October 2016 (**Paper II**). However, *Nitrospira sp.* was not observed in high abundance in all biofilms samples. Ammonia-oxidizing archaea, ammonia-oxidizing bacteria and nitrite-oxidizing bacteria are ubiquitous in marine water and well-adapted to low substrate concentrations and able to tolerate low oxygen environments (Lucker et al., 2010; Lucker et al., 2013; Park et al., 2010; Urakawa et al., 2006) which may assist in explaining their abundance in the biofilms, having a large range of DO concentrations. Besides typical AOB and NOB, genus *Brocadia sp.* affiliated to the group of the anaerobic ammonium-oxidizing bacteria (anammox) was detected in the biofilm. In biofilm samples taken in the period 2015-2017, genus *Scalindua sp*., typical marine anammox bacteria (Schmid et al., 2007), were observed in high abundance.

Biodeterioration of concrete associated with the nitrifying bacteria activities has been observed in various concrete infrastructures (Cwalina 2008; Noeiaghaei et al. 2017). In the Oslofjord tunnel, ammonia-oxidizing *Nitrosopumilus sp.,* AOB and NOB may have locally contributed to acidification and the deterioration of the sprayed concrete.

Furthermore, heterotrophic bacteria within *Kordiimonas, Woeseia, Rhodothermus and Euryhalocaulis* were detected in high abundance in biofilm samples (Figure 18). They were presumably utilizing the bioavailable fraction of dissolved organic matter in the water and/or organic matter originating from the biofilms. In the study preformed in the period 2015-2017 (**Paper II**), several SVs, *Kordiimonas, Marinicella, Parvularcula, Phycisphaera,* and *Bythopirellula,* were observed in high abundance. In the initial study (**Paper I**), the archaeon *Methanobacteria* sp. was observed in two SVs of a few biofilm samples with relative abundances <4%. The presence of methanogenic archaea suggesting that anaerobic zones occurred in the biofilm even though we could not observe it with microsensor measurement.

The genus *Mariprofundus* sp., within *Zetaproteobacteria*, were present in high abundance in some biofilms samples especially at the Pump station site (relative abundance <4.1%). The marine iron-oxidizing bacterium (IOB) *Mariprofundus* sp. oxidizes Fe(II) to Fe(III) at microaerophilic conditions, at which abiotic iron oxidation is of limited importance. The typical twisted stalks of *Mariprofundus sp*. was also observed in biofilms by the SEM-EDS point analysis preformed in 2016 (Karačić et al., 2018). The presence of IOB helps in explaining the observed steel fiber corrosion in the sprayed concrete, the orange/rusty biofilm colour, and the high iron concentration in biofilms (Table 4).

Since previous analysis by SEM showed presence of microbes with sheathed morphologies and chemical analysis of dark/black biofilms has shown manganese containing biofilm (Table 4), the presence of manganese-oxidizing bacteria (MOB) such as *Leptothrix* was expected. However, taxonomic analysis of biofilm samples from the Oslofjord subsea tunnel, based on the 16S rRNA gene sequences, did not reveal the presence of any known MOB. Biogenic manganese oxidation has been detected without identification of any known MOB based on 16S rRNA genes, suggesting that manganese oxidation could be performed by different groups

of microorganisms, not only restricted to the phylogenetically group of established MOB (Cao et al., 2015). In the initial study of microbial community composition (**Paper I**), OTU200 identical to *Geobacter* sp. M168B-09 (Blast, Genbank: AB721177), capable to reduce precipitated Fe(III) and Mn(IV) when oxidizing organic matter, was detected in a several biofilm samples. Putative SRB within *Desulfobacterales* were also observed in the biofilm samples from 2015 and 2016 (**Paper I** and **II**).

SRB would have been an indication of sulphur cycling, which leads to concrete degradation (Satoh et al. 2009). But since these OTUs / ASVs could not be assigned at higher precision than order (*Desulfobacterales*), their function remains unknown.

Interestingly, many of the OTUs / ASVs could not be assigned to any genus or species, just like in most studies in marine environments using high throughput sequencing methods (Bech et al., 2020).

4.3.2 Microbial community composition of Mesocosms biofilms

Similar to the microbial community composition of biofilm samples from the Oslofjord subsea tunnel, microbial community of the mesocosms biofilms contained high abundances of microorganisms affiliated to the phyla *Proteobacteria, Planctomycetota, Bacteroidota, Verrucomicrobiota, Actinobacteriota, Chloroflexi, Myxococcota* and *Bdellovibrionota.* The 20 most abundant taxa, grouped by order, are presented in Figure 19. Similarity between microbial composition of mesocosms and tunnel Oslofjord biofilms was observed.

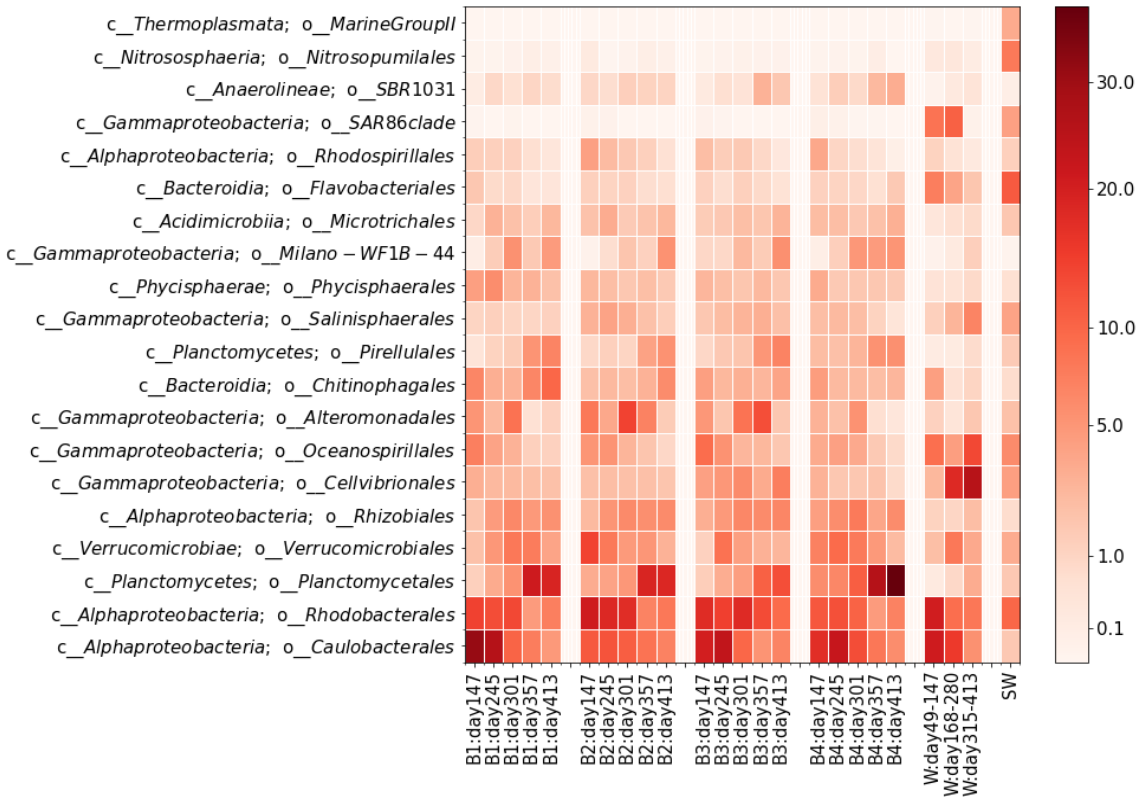

Figure 19. The 20 most abundant orders in the microbial communities. The colour bar indicates percentage relative abundance in the samples. For the biofilms (B1-B4) triplicate samples were merged. The water samples were merged into three groups representing the early phase (day 49-147), the middle phase (day 168-280) and the later phase (day 315-413). For the sea water (SW), all samples were merged.

Microorganisms belonging to *Caulobacterales* and *Rhodobacterales* were detected in high abundance in all mesocosms biofilm and water samples. Decrease in relative abundance over time was observed for these microorganisms, while increasing trends were observed for *Planktomycetales*, *Rhizobiales*, and *Pirellulaes* orders. Similar temporal trends for the mentioned orders were seen in the water samples. However, several orders such as *Cellvibrionales*, *Salinisphearales*, *Flavobacteriales* and *SAR86 clade* was observed in higher relative abundance in the water samples in comparison to the biofilm sample from the four mesocosms systems. Some orders, such as *Marine Group II* and *Nitrosopumilales,* was detected in high relative abundance in the sea water samples but they did not remain the mesocosm systems. However, similar to microbial composition of biofilm samples from the Oslofjord subsea tunnel, most ASVs detected in the mesocosms biofilms communities could not be assigned to either family or genus level. In order to understand the roles of the major contributors in environmental biofilm samples, complementary methods such as metagenomic analysis and/or advanced enrichment and isolation studies are needed.

4.4 How are the microorganisms distributed?

4.1 Alpha diversity of microbial communities

In **Paper II**, alpha-diversity was measured as taxonomic richness and evenness of the total biofilm microbial communities from March 2015-November 2016 from three tunnel locations. (Figure 20). The richness was significantly different between the sites (Welch's test, $p<0.001$), with Test site having significantly higher richness than the Main tunnel and Pump station (post-hoc, Games-Howell, $p<0.001$). However, evenness was rather similar between three tunnel locations with no significant differences.

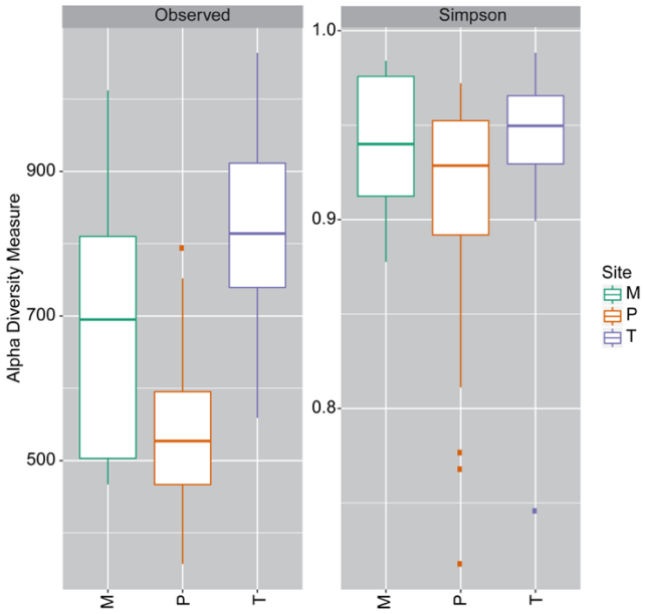

Figure 20. Richness as observed number of SVs and Simpson's evenness of the total microbial communities from March 2015-November 2016 from three tunnel locations. The boxes show median, 25 and 75 percentiles. The vertical lines show minimum and maximum values excluding outliers, and the dots show outliers.

In the timeline study presented in **Paper III**, alpha diversity was measured at the diversity order of 0 (^{0}D), equivalent to richness giving equal weight to all ASVs, and 1 (^{1}D), taking the relative abundances of the ASVs into account.

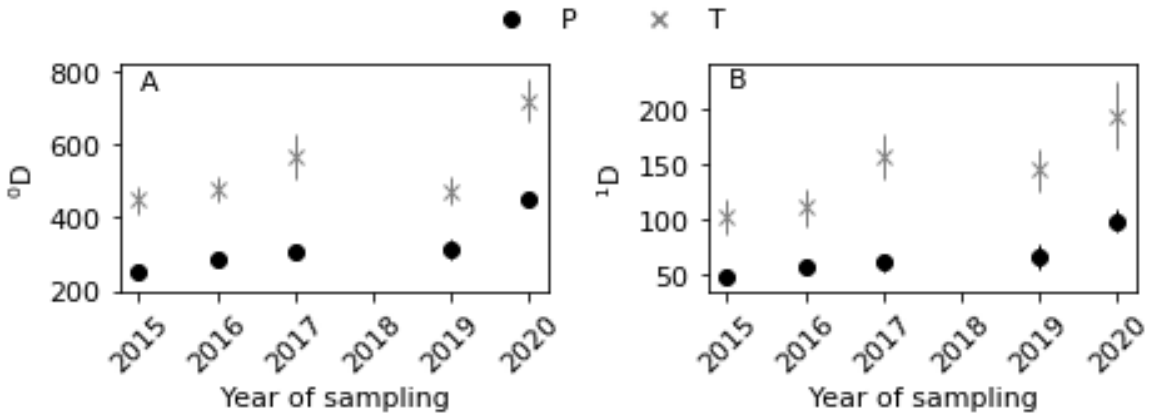

Figure 21. Alpha diversity of biofilm samples at the Pump station (P), and Test site (T) sampled in period of 2015-2020. Diversity (D) as Hill number with diversity order 0 (A) and 1 (B).

Alpha diversity of the Pump station and Test site biofilm communities were increased over time for both diversity orders, with particularly high values observed in the biofilm samples taken in September 2020 (Figure 21). Interestingly, biofilm that had existed for almost 20 years, still show patterns of increasing alpha diversity.

The same pattern of linear increase of alpha diversity over time was observed in the mesocosm biofilm communities across all four experimental systems for both ^{0}D and ^{1}D (ANOVA, $p<0.001$ and $p<0.01$, respectively) (Figure 22). Although alpha diversity was also different between the four types of biofilm (B1-B4) for both ^{0}D and ^{1}D (ANOVA, $p<0.01$), post-hoc testing could not separate the biofilm types (Games-Howell, $p>0.05$). Alpha diversity of seawater microbial communities was higher compared to the planktonic communities in the water samples for both diversity orders ^{0}D and ^{1}D.

Several studies of biofilm communities have shown linear increases of richness and alpha diversity over time (Redford & Fierer, 2009; Veach et al., 2016) which follows general patterns of species-time relationships observed in many microbial ecosystems (Shade et al., 2013).

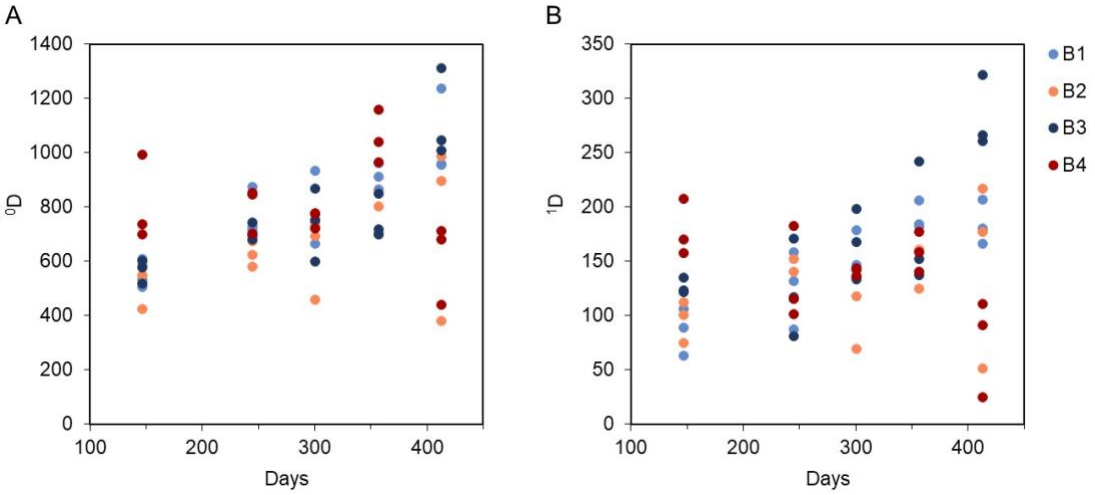

Figure 22. Alpha diversity of the mesocosms biofilm samples over time for the four different treatments (B1-B4). Diversity (D) presented as Hill number with diversity order 0 (A) and 1 (B).

4.5 Does microbial community differ between tunnel sites?

The beta-diversity of the biofilm communities from the three Oslofjord subsea tunnel sites, visualized with PCoA based on Hill number with diversity order ^{0}D, showed dissimilarities of microbial communities of biofilms sampled during period of five years, 2015-2020, (**Paper IV**) (Figure 23). This was confirmed by Permanova, showing that three locations had microbial community structures that were significantly different to each other. Although differences in community structure between the three tunnel locations were evident, the composition of the biofilm communities were comparable with many shared abundant taxa (Figure 18).

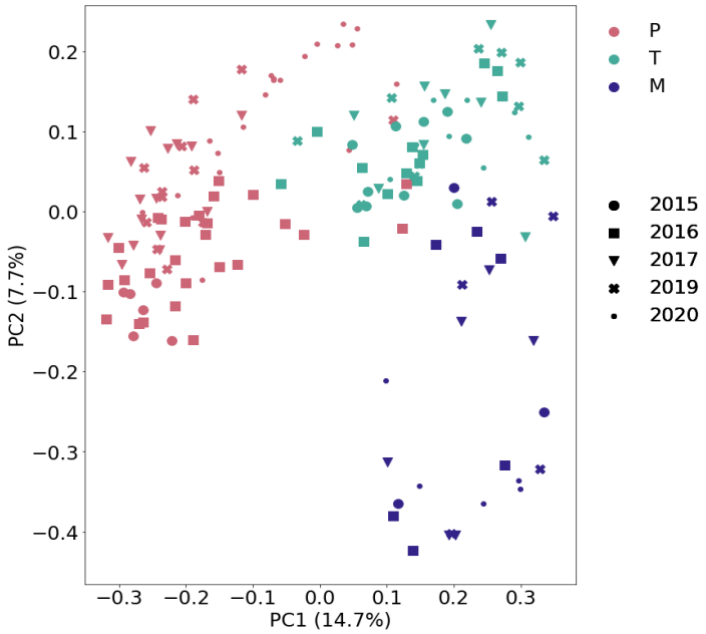

Figure 23. PCoA plot show significant difference in biofilm community of tunnel sites: the Pump station (P), the Test site (T) and the Main tunnel (M).

4.6 How do concrete characteristics affect biofilm formation and microbial community composition?

Microbial colonization of cementitious materials submerged in seawater is influenced by concrete composition and surface roughness. Surface roughness has been determined as the most important physical factor for biofilm formation on concrete in marine environment (Gaylarde, 2020). Many studies show that surface roughness has large effect on microbial colonization of different material and in different environments (Hayek et al., 2021).

In the mesocosm study, the steel fiber reinforcement was found to have a greater effect on the biofilm community composition than the surface roughness. The biofilm samples on PCoA plot were clustered based on the presence/absence of steel fibers in the concrete (Figure 24A). The dissimilarity between biofilm samples collected from the concrete surface with/without steel fibers were consistently significantly higher than the dissimilarity between biofilm samples from rough and smooth concrete surface, which in turn was had higher dissimilarity that replicate samples (Figure 24B).

Significant difference in microbial biofilm composition between the four mesocosms systems (p=0.0001, Permanova) was observed, but all biofilm communities followed a similar temporal trajectory (Figure 24A). To investigate how steel fiber content, concrete surface structure and time affect the abundance of individual taxa in the biofilms, DESeq2 analysis was used (Love et al., 2014). Significant difference in abundance based on the concrete surface structure was observed for only 10 ASVs, while 38 ASVs had significant differential abundance based on the presence/absence of steel fiber reinforcement in the concrete samples (Figure 25). Most of the ASVs, that had higher abundance on concrete samples with steel fibers, have unknown roles in the biofilm community

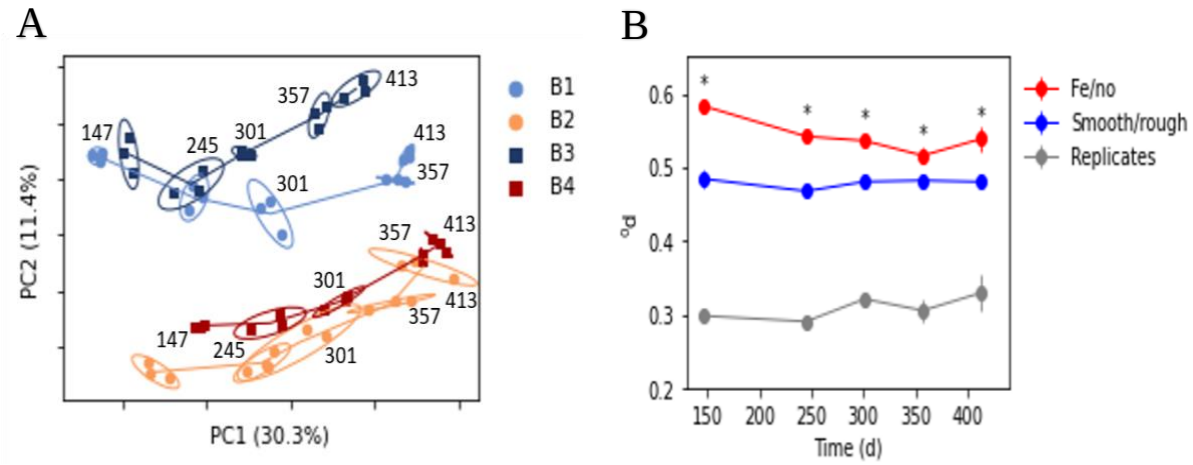

Figure 24. Beta diversity based on ^{1}d dissimilarities. PCoA of the biofilm samples, where the ellipses encircle replicate samples from the same time point (A). The time point (day of the experiment) is denoted at each ellipse. Dissimilarities between the biofilm samples of replicates (grey), concrete surfaces with different roughness (blue), and concrete with and without iron fibers (red (B)). The average and standard error of pairwise dissimilarities is shown. Asterisks (*) indicate that that the dissimilarity between samples from concrete with and without iron fibers is significantly greater than the dissimilarity of samples from concrete with different roughness ($p<0.05$, Welch's t-test).

Some of the taxa that appeared to favour steel fiber reinforced concrete were *Magnetospiraceae*, *Portibacter*, *Rubripirellula*, and *Rhodopirellula*. Interestingly, the typical marine iron-oxidizer *Mariprofundus* was not enriched on the steel-fiber containing concrete samples. However, *Mariprofundus* was presented in several biofilm samples from concrete without steel fiber reinforcement (System 1). Instead, an ASV286 within *Magnetospiraceae* was significantly more abundant in biofilms on steel reinforced concrete samples. This taxa had high relative abundance in the first sample taken on day 147 and then decreased over time. *Magnetospira* species are known to be involved in iron oxidation and/or reduction of iron oxides (Schüler & Frankel, 1999). This may suggest that ASV286 contributed to iron oxidation in the early stage of biofilm development and then decreased in relative abundance when most of the exposed iron surface had been converted into iron oxides (Figure 26). Additionally, ASVs within genus *Portibacter*, *Rubripirellula*, and *Rhodopirellula*, had high abundance in steel-fiber reinforced concrete samples although they were also present on concrete without steel fibers. *Portibacter* has previously been found to thrive on iron slag (Ogawa et al., 2020) and *Planctomycetes*, which include *Rubripirellula* and *Rhodopirellula*, have been found in iron-hydroxide deposits in marine habitats, suggesting that these microorganisms may be involved in iron metabolism (Storesund & Øvreås, 2013)

Figure 25. ASVs with significant differential abundance based on DESeq2 results (padj < 0.001). Positive log2 fold change means that the ASV increased in abundance with time (black squares), had higher abundance on steel fiber containing surfaces (red circles), or had higher abundance on smooth surfaces (orange X). Each point represents one ASVs. They are grouped based on genus classification on the left y-axis. The right y-axis shows taxonomic order. The red/pink and blue/light blue bars on the right x-axis shows how the orders are grouped into classes and phyla, respectively. If a point is surrounded by a blue circle, it means that ASV had a significantly higher abundance in the biofilm in comparison to the water samples (padj < 0.05).

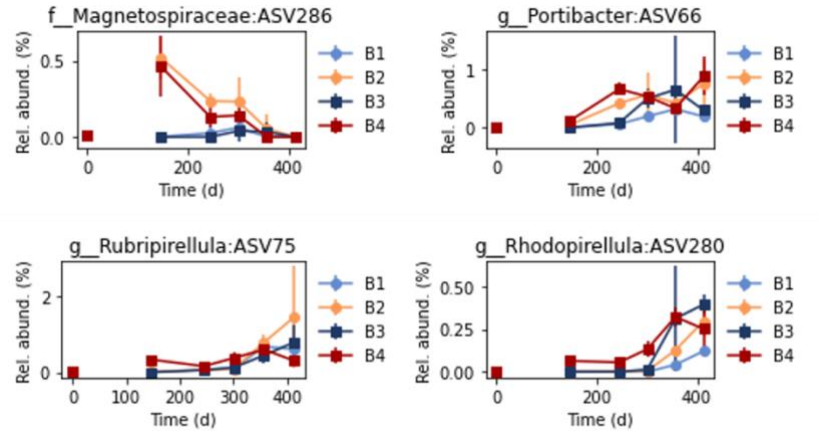

Figure 26. Relative abundance of some ASVs with significantly higher abundance in biofilms on steel-fiber containing concrete. The point at time 0 is the relative abundance in seawater samples. Error bars show standard deviations of triplicate samples.

In order to understand how concrete structure effect microbial communities composition in the subsea tunnels, concrete blocks with/without steel reinforcement were kept for one year (2019-2020) in Ditch A at the Test site. After one year, the biofilm communities developed on the concrete blocks with steel fibers were different compared to the biofilms formed on concrete without reinforcement (Figure 27).

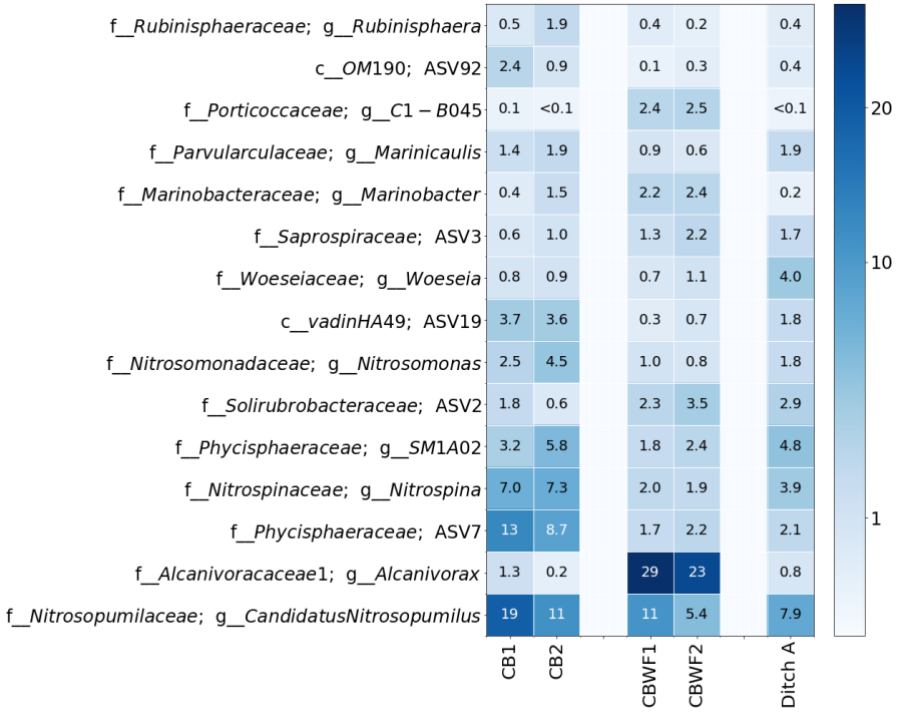

Figure 27. Heatmap showing 15 most abundant taxa in biofilm communities. Triplicate samples were merged. CB1&CB2- concrete blocks without fibers reinforcement; CBWF1& CBWF2 – concrete blocks with steel fibers; Ditch A- water from the ditch A

The most abundant taxa of one-year old biofilms concrete blocks were *Nitrosopumilus* sp., *Alcanivorax* sp., *Nitrospina* sp., *Nitrosomonas* sp., and ASV7, SM1A02, ASV2, ASV19, ASV3 taxa. It was found that many taxa were shared with microbial communities from the ditch water. Several taxa such as *Alcanivorax* and *Marinobacter* had much higher abundance in the biofilms formed on reinforced concrete.

4.7 Is there any difference between biofilm and planktonic microbial communities (Paper IV)?

PCoA plot based on Hill number diversity ^{1}d revealed that the biofilms formed on the concrete surfaces in the mesocosm study, the planktonic microorganisms in the water that had percolated over the concrete blocks in systems and the planktonic microorganisms in the seawater formed three distinct microbial communities (Figure 28). Significant differences between the three groups were confirmed with Permanova (p=0.0001). Although all sample types shared many ASVs, the relative abundance of the sequence reads differed. However, only 7 ASVs had significantly higher abundance in the water than in the biofilm, while 81 ASVs were more abundant in the mesocosms biofilms (p<0.05, DESeq2).

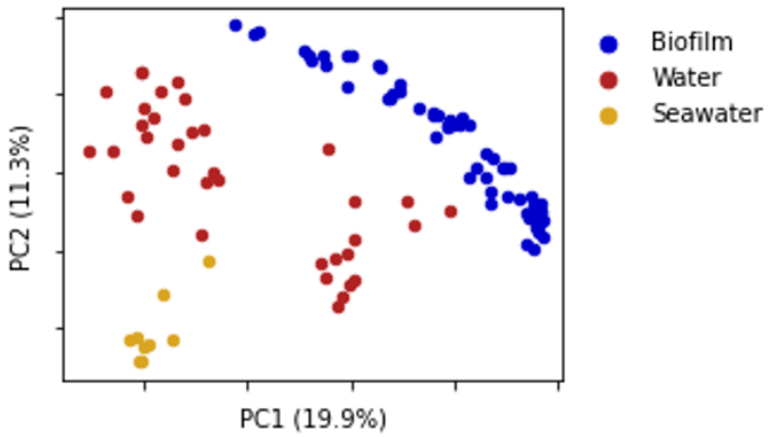

Figure 28. PCoA plot showing separation between microbial communities from the mesocosms biofilm, water and seawater samples. Beta diversity based on ^{1}d dissimilarities.

4.8 How does microbial communities change over time?

4.8.1 Temporal dynamics of Oslofjord subsea tunnel biofilms (Papers II-III)

The changes in appearance and in observation of different microorganisms being present from 2004 to 2020 suggest temporal dynamics in the Oslofjord subsea tunnel biofilms. To systematically investigate temporal microbial dynamics, sampling was performed during a period of five years (2015-2020). To investigate beta diversity over time, the dissimilarity values were plotted at increasing time differences. Although the slope was rather flat for both ^{0}d and ^{1}d, longer time differences between two samples correlated with higher dissimilarity, indicating a slow and gradual succession of the biofilm communities (Figure 29).

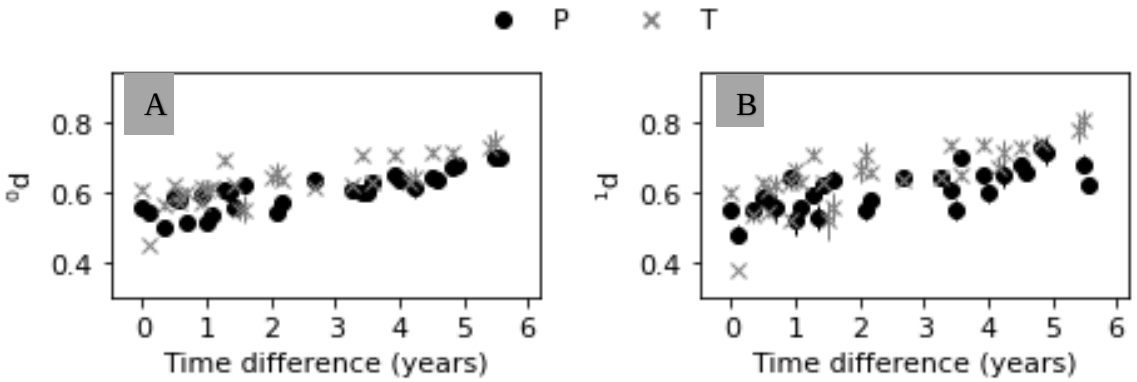

Figure 29. Dissimilarity between biofilm communities analysed at different time points analysed using Hill-based indices with diversity order 0 (A) and 1 (B). Average values for each year and time difference are shown. The error bars represent the standard error of the mean.

In **Paper II**, temporal dynamics of the microbial communities was observed even in a period of less than one year (November 2015-October 2016) at the Pump station ($p = 0.002$), and to some degree at the Test site ($p = 0.043$), while for the Main tunnel, no clear changes in microbial community were observed ($p = 0.61$) (Table 5).

Table 5. PERMANOVA based on Sørensen dissimilarities to test for differences in microbial community structure. P = Pump station, T = Test site, M = Main tunnel.

	df	SS	MS	Pseudo F	p
Between Sites (M, P, T)	2	2.05	1.02	9.61	0.001
Residuals	61	6.50	0.11		
Total	63	8.55			
Between occasions, T	2	0.29	0.14	1.49	0.043
Residuals	20	1.93	0.097		
Total	22	2.22			
Between occasions, M	1	0.98	0.098	0.84	0.61
Residuals	7	0.82	0.12		
Total	8	0.91			
Between occasions, P	2	0.53	0.26	2.70	0.002
Residuals	29	2.84	0.098		
Total	31	3.37			

df = degrees of freedom; SS = sum of squares; MS = mean squares; Pseudo F = F value by permutation, p-values based on 999 permutations.

The differences in biofilm microbial community at the Pump station location were visualized with NMDS ordination (Figure 30), which illustrates that the biofilm composition at the Pump station was in fact dynamic even within a time frame of less than a year.

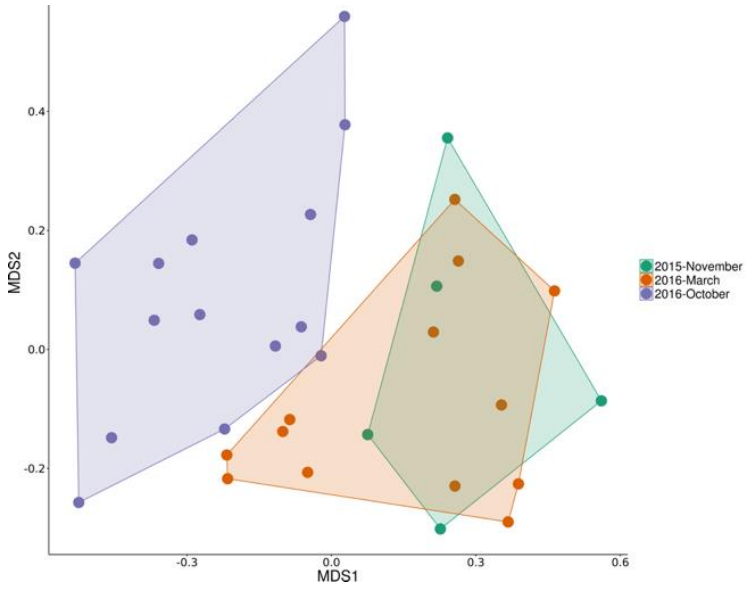

Figure 30. NMDS ordination shows significant difference in biofilm community at the Pump station from November 2015 until October 2016.

Temporal dynamics of microbial communities at Pump station location in period of five years (2015-2020) was confirmed with PCoA plot based on ^{1}D beta-diversity dissimilarities (Figure 31) (**Paper III**). The observed microbial community dynamics over time at the Pump station was associated with higher water flow at this location. The flow of saline groundwater was greater at the Pump station then at the other sites. It is known that differences in water flow rates affect the transport of nutrients and diffusion gradients within the biofilm (Stewart, 2003) which influence the microorganisms within the biofilm. Additionally, higher immigration of planktonic microorganisms from the saline groundwater could be expected, which should affect the biofilm community composition (Flemming et al., 2009).

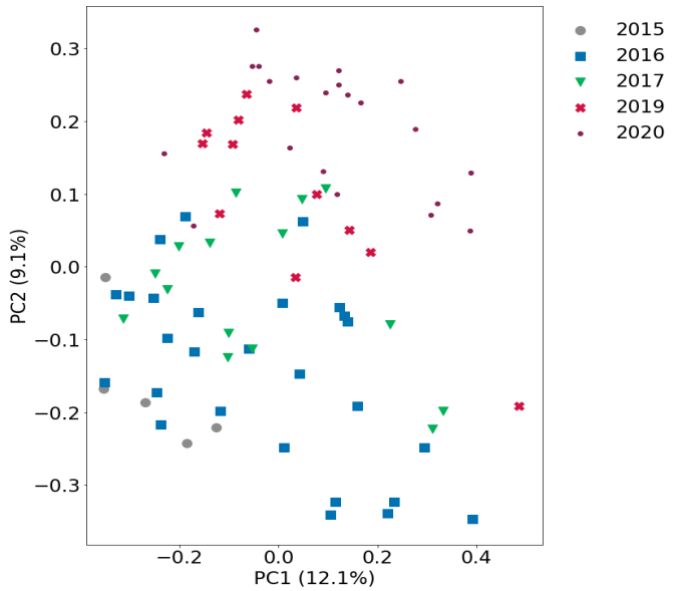

Figure 31. PCoA based on ^{1}D beta-diversity dissimilarities show significant change of microbial biofilms at the Pump station locality sampled in 2015, 2016, 2017, 2019 and 2020.

This might explain the fast development of biofilm microbial community at the early stage (2004-2005), when the water flow was considerably lower as well as differences in the concrete biodeterioration. Later on, when flow increased, the environmental conditions apparently became less aggressive, with higher pH and less leaching of Ca from the concrete. Besides, the salinity of interacting waters appears to have increased in the period 2004-2016, which by itself is a sign of sustained aggressiveness (Karačić et al., 2018). Additionally, increased water flow may lead to enhanced erosion in an already weakened subsea tunnel concrete surface.

4.8.2 Temporal dynamics of Mesocosms biofilms (Paper IV)

Biofilm communities and planktonic microbial communities from the four mesocosm systems followed a temporal trajectory (Figure 32A). It was observed that time was an important parameter affecting biofilm community composition in the mesocosms. Figure 32A shows that higher dissimilarity is correlated with longer time difference between two biofilm sampling occasions.

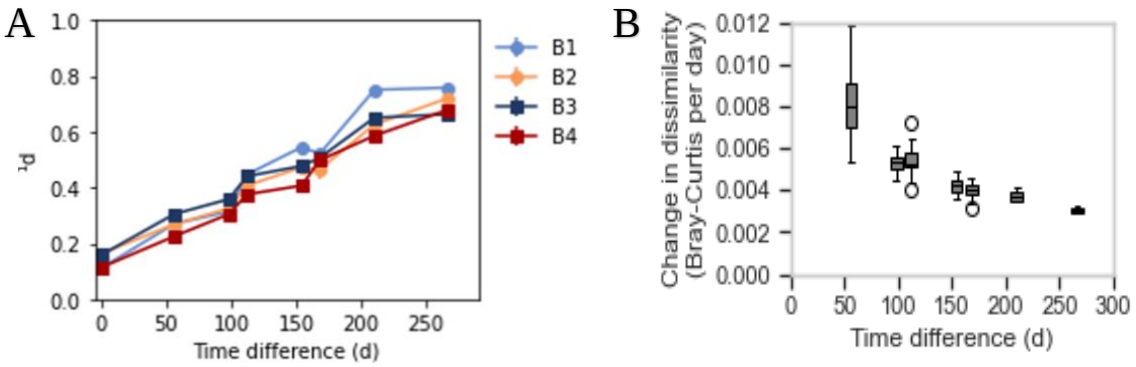

Figure 32. (A) The effect of time difference on dissimilarities. Each point shows the average of several pairwise dissimilarities. Error bars show standard error (too small to be seen in the graph). At a time difference of 0, the ^{1}d represents dissimilarity between biological replicates. (B) Box plots showing the rate of change in microbial community composition in Bray-Curtis dissimilarity per day for samples collected from biofilms in the same system but at different time points

The temporal rate of change in biofilms community composition was determined by dividing the dissimilarity between a pair of biofilm samples from the mesocosm system with the time difference in days between the sampling occasions (Figure 32B) (**Paper IV**). The Bray-Curtis dissimilarity index was used to allow comparison to previous studies of temporal microbial community dynamics in various environments and it gives weight to the relative abundance of ASVs (Shade et al., 2013). The observed rates were the same as those determined for microbial communities in lakes, freshwater streams, air, wastewater treatment plants, marine environments, soil, flowers, and humans (Shade et al., 2013).

4.9 How do microorganisms colonize the concrete surfaces?

4.9.1 Biofilm development on concrete in the mesocosm experiment

The microbial colonization of concrete and biofilm development are complex processes that are affected by many factors, such as environmental conditions, the microbial properties and the physical and chemical characteristics of the material surface (Hayek et al., 2021). Several

studies have shown that biofilm formation in different ecosystems is not random and it depends of species traits (Ali et al., 2019; Besemer et al., 2012).
The biofilm communities on concrete in the mesocosm were distinctly different from the planktonic communities in the flowing water and the seawater as shown on Figure 33 (**Paper IV**). It was observed that several taxa had higher abundance in the biofilms than in the water and had decreasing trend over time (Figure 19). This observation indicates that these microorganisms were early colonizers of the concrete in the mesocosm. Early colonizers are of great importance, because after adhering to the concrete surface, they provide conditions for colonization of subsequent microorganisms and influence the succeeding stages of biofilm formation. The relative abundance of early colonizers decreases over time because of competition for resources with later bacterial colonizers. Early colonizers observed in mesocosm study were affiliated to *Chitinophagales*, *Bacteroidia*, *Blastopirellula*, *Pirellulales Pir4 lineage*, *Ponticaulis*, *Hyphomonadaceae*, *Roseobacter*, *Glaciecola*, *Paraglaciecola*, and *Leptospiraceae* (Figure 33).

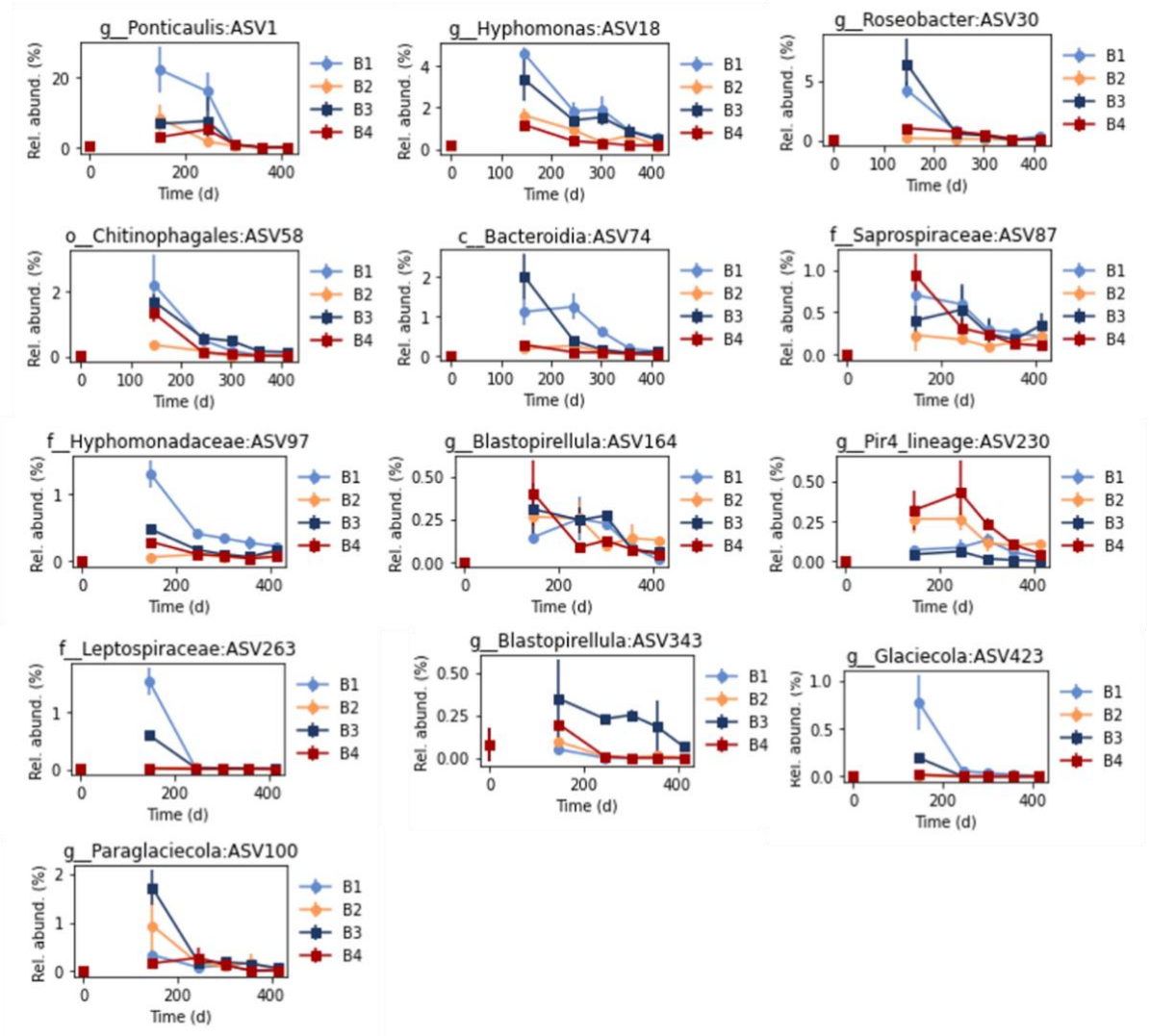

Figure 33. Relative abundance of early colonizers. The point at time 0 is the relative abundance in seawater samples. Error bars show standard deviations of triplicate samples.

The genus *Ponticaulis* was detected in high abundance in the all biofilm samples and has previously been found to play an important role in colonization and biofilm formation on steel in marine environments (Procópio, 2020). Several ASVs within the phylum *Planctomycetota*

increased over time in the biofilm samples from the mesocosm. Particularly ASV3 affiliated to genus *Planctomicrobium*, became dominant in mesocosms systems 1, 2, and 4, reaching over 30% relative abundance. Interestingly, the strain *Planctomicrobium piriforme,* was isolated from boreal lake and it was not able to grow at NaCl concentrations above 0.5% (Kulichevskaya et al., 2015). ASV3 had 87.75% nucleotide identity to this strain. However, a BLASTn search of NCBI Genbank resulted with 100% match with nucleotide identities from both wastewater treatment systems (LR637872.1) and coastal seawater (JF948432) suggesting that this ASV3 represented a species that can grow in many different environments.

For several taxa, it was observed that one ASVs was replaced by other ASVs within the same genus or family. This indicates competitive exclusion where two species /ASVs within the same genus/family occupy similar environmental niches in the biofilm. It is observed that two ASVs, affiliated to *Hyphomonas*, showed significant changes with time. ASV18 decreased with time and had higher relative abundance on concrete without steel fibers while ASV105 increased with time and had higher relative abundance on concrete with steel fibers.

4.10 How do biofilm communities assemble?

A long-standing challenge is to understand ecological mechanisms governing the microbial community composition in natural ecosystems. Traditionally, these complex mechanisms have been grouped into stochastic and deterministic factors (Widder et al., 2016). Stochastic factors include unpredictable disturbance, probabilistic dispersal and random birth-death events (Zhou & Ning, 2017) whereas environmental conditions, species traits and interactions are considered as deterministic factors (Chase & Leibold, 2009). Since natural environments consist of a large diversity of microorganisms with integrations and processes that are hard to predict and separate from random processes, knowledge about the detail mechanisms involved in biofilm formation in natural ecosystems is limited. Interestingly, only few studies have investigated biofilm succession in natural ecosystems.

To shed light on microbial community assembly mechanisms in the Oslofjord tunnel biofilms, standard effect size (SES) based on null-models were used (Chase et al., 2011; Stegen et al., 2012) in **Paper II**. The variation between the samples within each Oslofjord tunnel location (M_M, T_T, S_S), was lower than predicted by chance, while the variation between sites (M_P, M_T, T_P) was larger than predicted by chance (Figure 34).

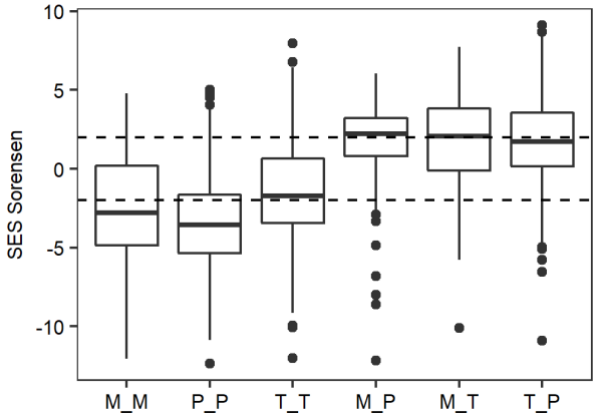

Figure 34. Standard effect size (SES). The hatched horizontal lines designate two standard deviations from the variation predicted by the null-model. The boxplot depicts the median (horizontal bold line); 25th and 75th percentiles (box delimiters); minimum and maximum values excluding outliers (vertical lines); and outliers (dots).

SES suggests that deterministic factors were important for shaping the biofilm microbial communities at the three Oslofjord subsea tunnel sites. It has been shown that niche differentiation caused by differences in water flow are important for microbial community assembly (Besemer et al., 2012). Therefore, in **Paper II** we hypothesized that the more stable and lower flow of water at the Test site location and the Main tunnel would enable the establishment of more niches driving selection for a biofilm that would harbour a higher diversity than the higher water flow at the Pump station location. However, the effect of water flow on biofilm community composition may not be caused only by deterministic factor selection (via niche differentiation), since stochastic factor such as dispersal of microorganisms from the water to the biofilm could also have considerable impact (Woodcock et al., 2013). Since stochastic dispersal refers to the passive movement of microorganisms among communities, at environmental conditions with heterogenous water flow and rough concrete surface as in the Oslofjord tunnel, it has failed to explain biofilm community assembly. For example, in free-floating biofilms in wastewater reactors and freshwater stream biofilms, the early stages of succession was influenced by stochastic factors, while niche-based deterministic factors were dominated in matured biofilms (Liébana et al., 2019; Veach et al., 2016).

In order to investigate mechanisms involved in the early stages of biofilm succession on concrete surfaces, the mesocosm experiment was performed (**Paper IV**). Microbial community assembly of the mesocosms biofilms was assessed using the Raup-Crick null model (Raup & Crick, 1979). Detail explanation of null-model used in this experiment can be found in **Paper IV**. Null model results for the incidence-based based dissimilarity index (^{0}RC) and relative abundance-based index (^{1}RC) are presented in Figure 35. The incidence-based based dissimilarity index (^{0}RC) shows 0 value for time differences less than approximately 150 days which means that when it comes to presence/absence of ASVs, the compositional similarity is much higher than what would be expected at random assembly processes. The results of relative abundance-based index (^{1}RC) show intermediate values, which means that the difference in relative abundance between the detected ASVs could be explained by random processes. At longer time intervals (>250 d), the ^{0}RC index has intermediate values or is close to 1 in some systems., whilst ^{1}RC is close to 1 in all systems. This means that there has been a significant change in the identity of ASVs and especially in the relative abundance of ASVs.

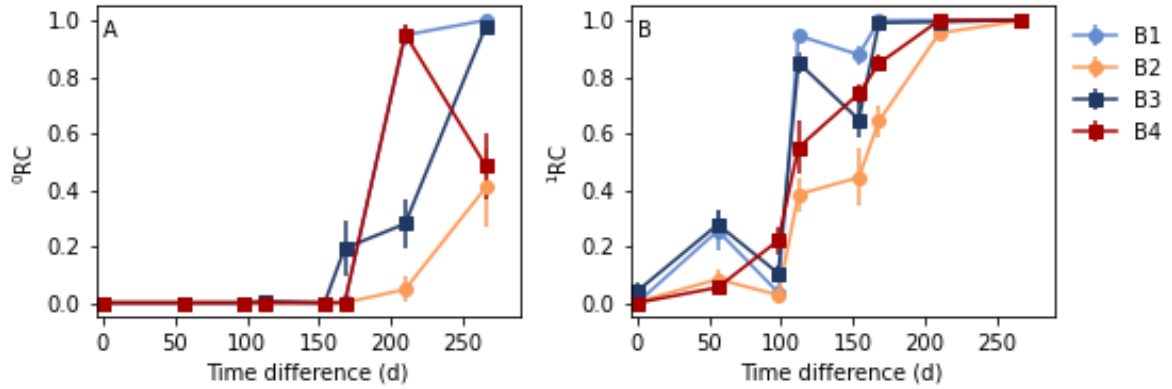

Figure 35. Null model results (^{q}RC) for the incidence-based based dissimilarity index (A, ^{0}d) and the relative-abundance based dissimilarity index (B, ^{1}d). The x-axis shows the time difference between the samples being compared. The average value of pairwise comparisons of samples from the same system are shown. The error bars show the standard error of the mean.

A comparison of null model results between mesocosms systems revealed that at all time points, the ^{0}RC was close to 0 and the ^{1}RC had intermediate values (**Paper IV**). These results suggest that it is primarily time that drives turnover (compositional differences) in mesocosms biofilm communities.

4.11 What is the metabolic potential of the Oslofjord subsea tunnel biofilms? (Paper III)

The relative abundance of the top 40 MAGs and their genes for iron oxidation, iron reduction, nitrogen- and sulfur metabolisms of selected biofilm samples from the Oslofjord subsea tunnel are presented Figure 36. Cyc2 is the key protein for iron oxidation in bacteria (McAllister et al., 2020). Well known iron-oxidizing *Zetaproteobacteria* were observed among other MAGs with the Cyc2 gene detected in the biofilm samples. The iron reduction predictions were made by looking at presence of porin-cytochrome clusters **(**porin, periplasmic c-type cytochrome and/or an outer-membrane c-Cyt) in the genome (Shi et al., 2014). These gene clusters may potentially be involved in Fe(III) and Mn(III, IV) reduction.

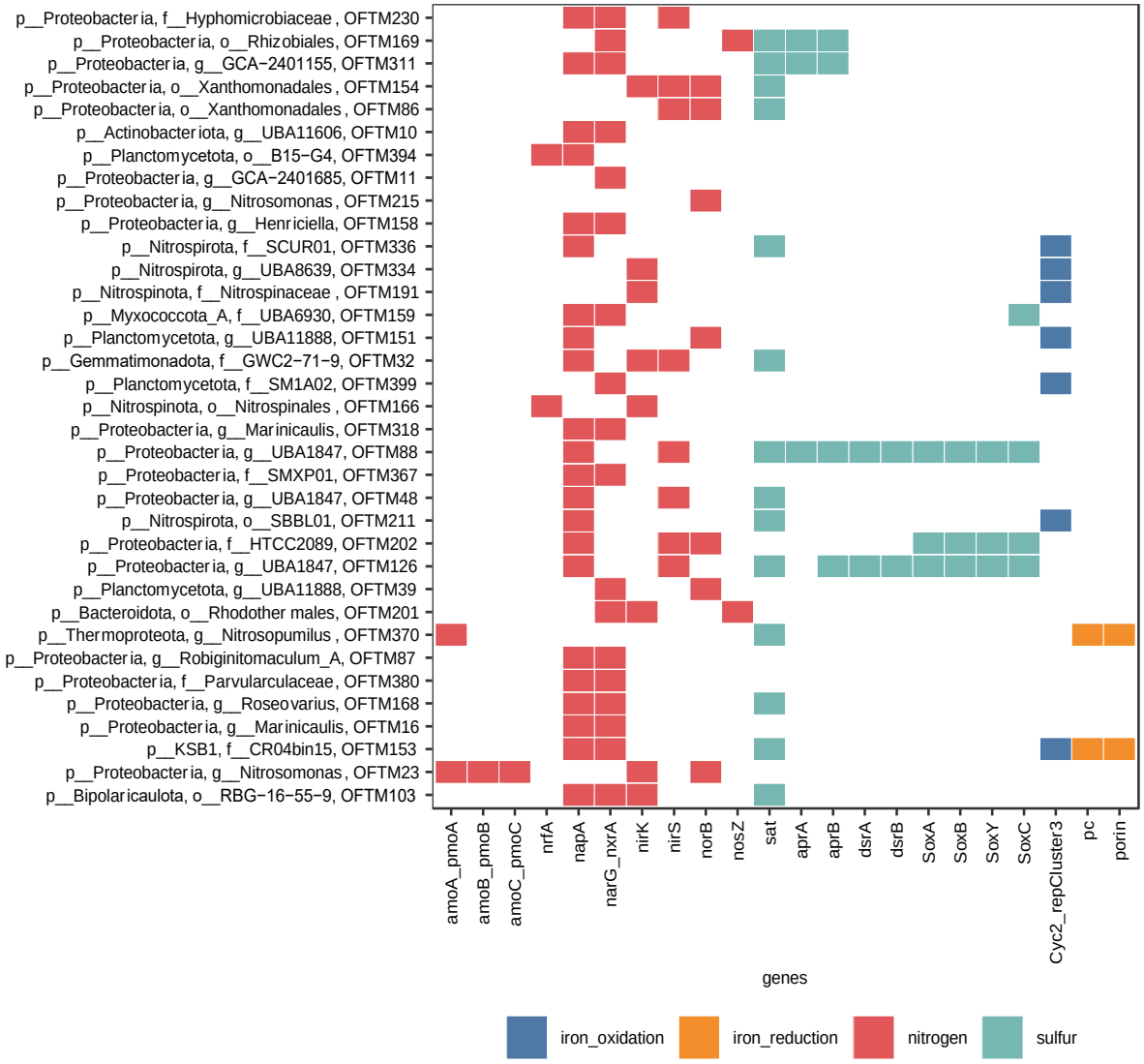

Figure 36. Abundance heatmap of the 22 genes for potential iron-oxidation, iron-reduction, nitrogen, and sulfur cycles in the top 40 MAGs.

Several genes were used for detection potential sulfur oxidisation/reduction (*Sat*: sulfate adenylyltransferase (sulfate to APS), *AprAB*: adenylylsulfate reductase (APS to sulfate), *dsrAB*: dissimilatory sulfite reductase (sulfite to sulfide), *SoxA ,B C, Y*: thiosulfate oxidation). The gene *dsrAB* can operate in the reductive direction (sulfite - sulfide), but sometimes sulfur oxidizing bacteria can use it in opposite direction (sulfite - sulfide). Actually, the oxidative and the reductive *dsrAB* are phylogenetically distinct, and thus it is possible to tell them apart. A phylogenetic tree of all the d*srAB* sequences from the Oslofjord tunnel biofilms shows that most MAGs with a *dsrAB* will likely use this gene for sulfur oxidation (Figure 37). The only detected sulfate reducing bacteria (SRB) in the study was OFTM352 affiliated to the *Thermodesulfovibrio*. Thus, relative abundance of SRB was only 0.05% of total community.

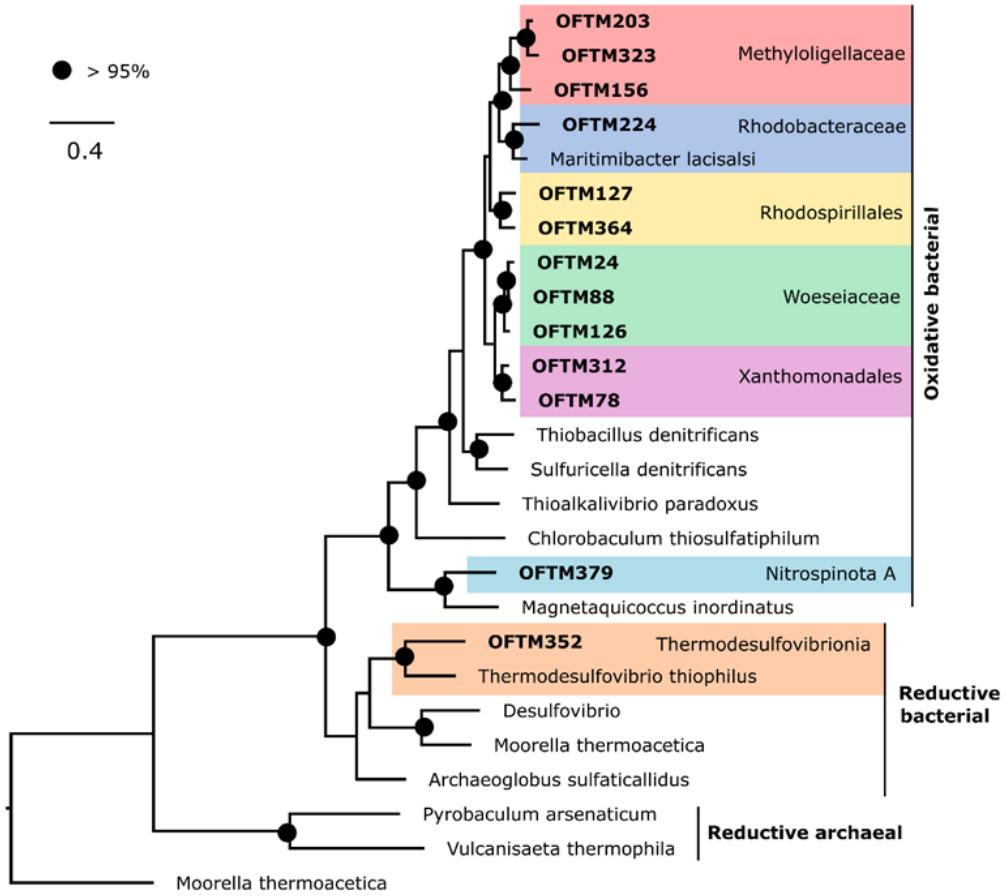

Figure 37. Phylogenetic tree of all dsrAB sequences of selected biofilm samples

In order to detect nitrogen converting microbes several genes were used: *nirA* and *nirB* (assimilatory nitrate reductases), *nrfA* (dissimilatory nitrate reductase), *napA*/*narG* (nitrate reductase), *nirk/nirS + norB + nosZ* (denitrification), *amoA* (ammonia oxidation) and *nxrB* (nitrite oxidation). The MAGs affiliated to the ammonia oxidizing archaea (AOA) and aerobic ammonia oxidizing bacteria (AOB) were observed in low abundance. Genes linked to denitrification were common within the constructed MAGs and 70% of the MAGs had a nitrate reductase (*Nar* and *Nap*), and hence could reduce NO_3^- to NO_2^-. Figure 38 shows abundance of denitrifying genes within constructed MAGs from the biofilm samples from two tunnel locations (the Pump station and the Test site).

Interestingly, within the *Nitrospirales* MAGs, several MAGs contained the Cyc2 gene (for potential iron/manganese oxidation). One cluster affiliated to the *Nitrospirae* belonged to

Manganitrophus cluster (Figure 39). Yu & Leadbetter (2020) showed that *Manganitrophus noduliformans* is chemolithoautotrophic manganese-oxidizing microorganism related to formation of manganese-oxide nodules. In this bacterium, manganese oxidation is proposed to be mediated by Cyc2 and other proteins. Presence and activity of *M. noduliformans* may explain formation of observed Mn-oxide nodules and Mn-biominerals (todorokite (predominantly Mn^{IV}), rhodochrosite ($MnCO_3$) and manganosite (MnO)) in the Oslofjord subsea tunnel biofilms and concrete.

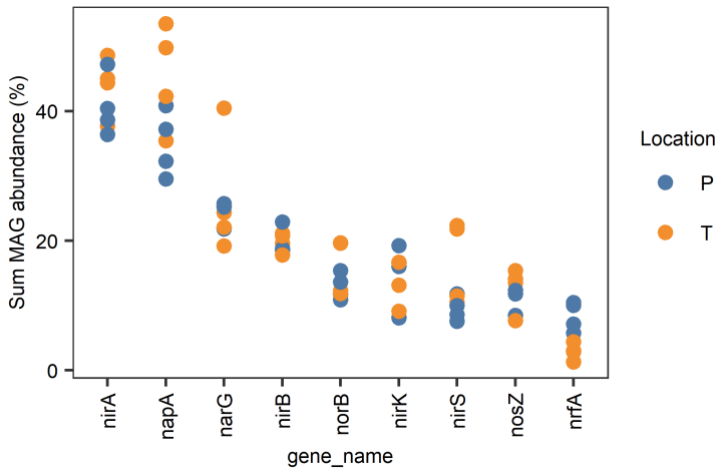

Figure 38. Abundance of denitrifying genes in the MAGs from the Pump station (P) and the Test site (T).

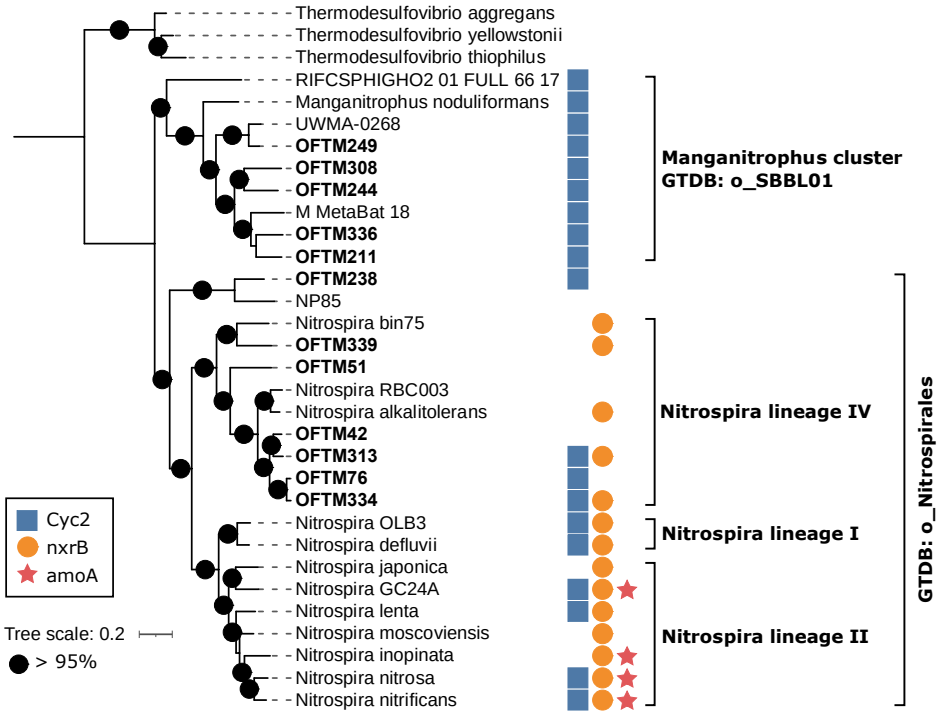

Figure 39. Phylogenetic tree of MAGs classified as *Nitrospiria*, based on 74 single copy genes. *Thermodesulfovibrio* was used as an outgroup. The tree scale represents amino acid substitutions per site

4.12 How does the biofilm look under the microscope?

In **Paper II**, SEM-EDS point analysis of biofilm sampled in 2016 confirmed presence of the iron-oxidizing twisted stalked bacteria *Mariprofundus* (points 1 and 2 in Figure 40; Table 6). *Mariprofundus sp*. oxidize iron at microaerophilic conditions and natural pH and excrete extracellular stalks rich in Fe during growth. Apart from twisted stalks (points 1 and 2 in Figure 40; Table 6), non-specific biomass (points 3 and 4) and anticipated mineral material (point 5) were observed with SEM. Observed stalks were particularly rich in iron, but even the non-specified biomass (3-4) contained a lot of iron compared to the anticipated mineral material, which was high in silicon, confirming its mineral nature.

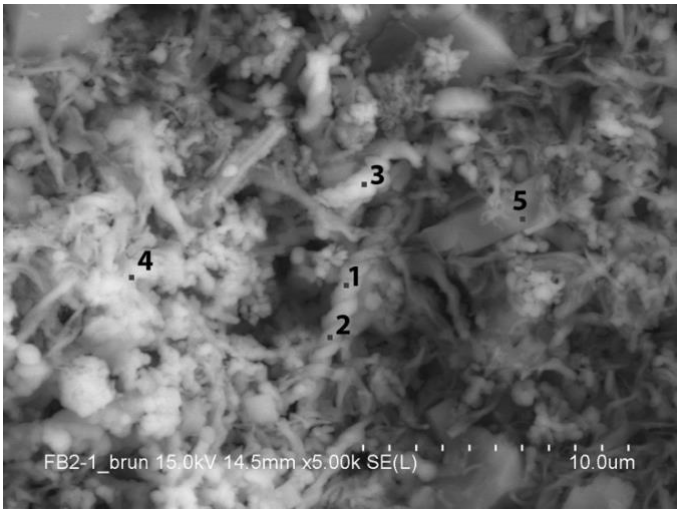

Figure 40. SEM micrograph with of biofilm biomass; magnification 10000×. Points 1-5 refer to measurements by EDS (see Table 6).

Table 6. Scanning Electron Microscopy with Energy Dispersive Spectroscopy (SEM/EDS) analyses (atomic %) of biofilm samples with suggested iron-oxidizing bacteria. Analysed points correspond to Fig. 39.

Anal.Pt.	***O***	***C***	***Fe***	***Si***	***Cl***	***Na***	***Ca***	***S***	***Mg***	***Mn***
1	20.05	24.83	37.59	7.07	3.64	1.68	2.30	0.46	0.38	0.52
2	22.45	32.48	28.00	6.82	3.06	1.93	1.85	0.58	0.47	0.67
3	28.66	27.56	25.13	9.36	2.86	1.76	1.67	0.40	0.53	0.27
4	37.70	30.63	18.40	5.10	2.46	2.70	1.31	0.41	0.44	
5	45.47	28.87	3.36	20.11	0.92	0.48	0.36			

Previous SEM analysis suggested presence of sheathed morphologies similar to the *Leptothrix* (**Paper II**), but no OTU similar to known MOB were detected. SEM analysis of biofilms samples in September 2020 at Pump station site assessed Mn-nests, iron-rich filaments and iron-rich twisted stalks (Figure 41).

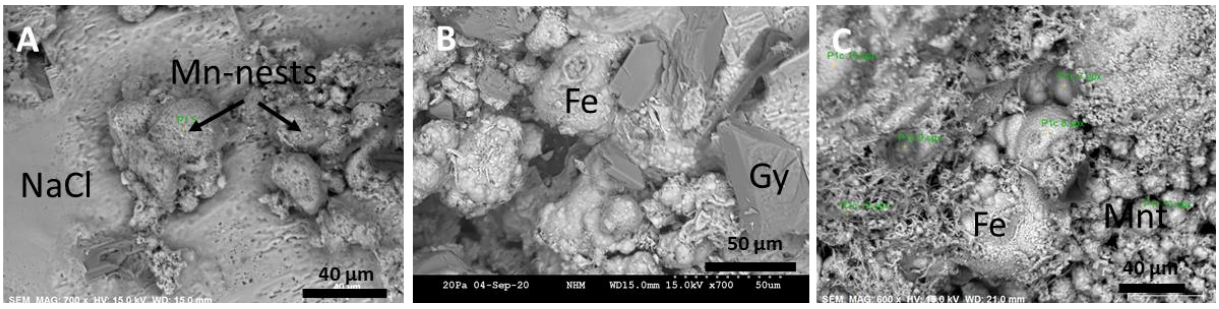

Figure 41. SEM images of biofilms and thin concrete layers beneath biofilms at the Pump station showing (A) Mn-biofilm (globules); (B) Deposits of Fe-rich nodules (Fe) and gypsum (Gy) on degraded sprayed concrete; and (C) Fe-rich filamentous material ad Mn-rich nodules.

In the mesocosm, biofilms sampled on concrete with fiber reinforcement after 357 and 413 days of exposure, mineralised microbes and stalks rich in iron were predominant (**Paper IV**). However, manganese globules were not observed in analysed samples (Figure 42).

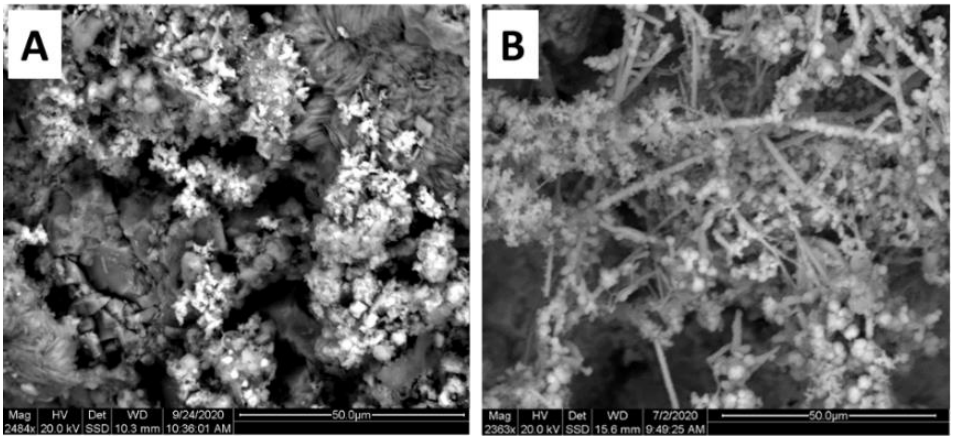

Figure 42. SEM-back scatter images: Surfaces of S4 after 357 (A) and 413 days exposure (B).

4.13 Concrete degradation products and biomineralisation in contact with saline water (Paper II- III)

SEM and XRD analysis of thin sections of concrete beneath the biofilms and biofilm material sampled in the autumn 2020 assessed the presence of buserite, todorokite and amorphous ferrihydrite at the Pump station and the Test site locations. Marcasite (FeS_2) was observed within thick biofilm at Pump station location. Additionally, thin section of concrete samples shows that leaching of calcium from the cement paste matrix underneath biofilm was common. The leached zone was characterised by Ca-depleted paste with Mg and S substitution and most notably dissolution of pre-existing thaumasite (Figure 43). Also, Popcorn calcite deposition (PCD) occurred in leached domains. It was evident that these degradation reactions were well developed at least 35 mm below the biofilms. This is in keeping with previous results from studies performed by Per Hagelia in the period 2004-2011 (Hagelia, 2007, 2011a, 2011b).
Mn-oxide and Mn-nodules were observed outside carbonate and brucite in outer deposits of concrete samples (**Paper III**).

Water chemistry analysis confirmed calcium dissolution from the sprayed tunnel concrete in contact with saline water (**Paper I,** and **Paper II**). Another evidence was precipitation of calcite, aragonite, Mg-calcite, magnesite and occasional gypsum just outside main water streams. Mn-oxide and Mn-nodules were observed outside carbonate and brucite in outer deposits of concrete samples (**Paper III**).

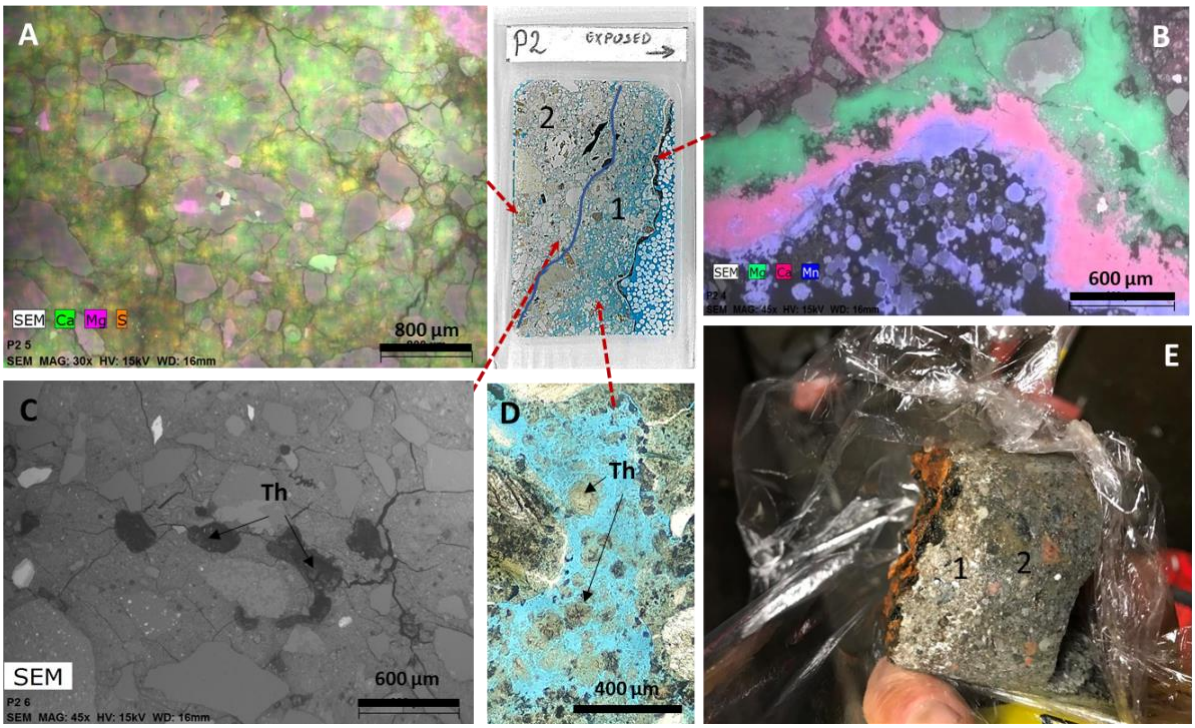

Figure 43. Thin section P2 with characteristic zonation and porosity shown with blue dye. Concrete and biofilm age about 21 years. *Zone 1:* Deposits of outermost Mn-oxide underneath Fe-rich slimy biofilm (not preserved in the thin section) with deposits of calcium carbonate derived from leaching of the cement paste, and inner magnesium silicate hydrate (MSH) (B). Most of Zone 1 was extremely porous, characterised by partial dissolution of pre-existing thaumasite (Th) (D: plane polarised light with blue dye showing secondary porosity). *Zone 2:* Ca-depleted cement paste substituted by Mg and S with extensive secondary shrinkage cracks (A) and occurrence of intact thaumasite (Th) in air voids towards Zone 1 (C). Image E shows the sprayed concrete core with layered Fe and Mn biofilm outside friable and leached outer Zone 1 and inner Zone 2.

5 Conclusions

The overall aim of this thesis was to increase the understanding of the mechanisms behind biologically induced degradation of sprayed concrete and accelerated corrosion of steel fibers in subsea tunnels caused by biofilm development. The approach has been to use a combination of sequencing methods to shed light upon the composition, diversity, and metabolic potential of this unexplored biofilm ecosystem, together with chemical measurements and visualization techniques to assess the chemical composition of the water, biofilm, concrete, and associated minerals within and underneath the biofilm.

The most important conclusions, with respect to the specific objectives, are as follows:

- Taxonomic analysis of the 16S rRNA amplicon sequences from 2015-2020 revealed that the microbial biofilm communities from different Oslofjord subsea tunnel locations had similarities in composition to other marine sediments and biofilms with high abundance of known nitrogen oxidizing bacteria, iron oxidizing bacteria, and several taxa of marine heterotrophic bacteria. However, many numerical important microorganisms could not be assigned to any known genus or species, just like in many studies in nature using high throughput amplicon sequencing. With metagenomic shotgun sequencing of selected samples we resolved 401 metagenome assembled genomes (MAGs), but only 145 MAGs were classified at the genus level using GTDB taxonomy, further highlighting that many novel species were present in the tunnel biofilms. The composition of the MAGs supported the findings by amplicon sequencing and complemented these with new taxa and metabolic functions in the biofilm (see below).
- The saline groundwater had a composition quite similar to the seawater with high concentrations of chloride, sodium, sulfate, and magnesium, while the concentrations of iron, manganese, and ammonium were generally low. In the biofilm, however, the concentrations of iron and manganese were high suggesting considerable formation of iron- and manganese oxides. Calcium, as well as magnesium, was also fairly abundant. The water in contact with the biofilm contained elevated concentrations of particularly calcium, suggesting leaching from the concrete. Within and underneath the biofilm, iron(III) and manganese(IV) biominerals such as ferrihydrite, buserite and marcasite was observed. There were clear signs of concrete degradation underneath the biofilm, as shown by calcium leaching and magnesium substitution of the calcium-silicate-hydrate (C-S-H) and popcorn calcite deposition.
- Within the biofilm, the concentrations of dissolved oxygen decreased with increasing biofilm depth suggesting varying environmental conditions throughout the biofilm. At lower waterflow, steeper dissolved oxygen gradients were observed, suggesting that the water flow was an important parameter controlling the environmental conditions within the biofilm.
- Temporal dynamics of microbial communities was observed at all tunnel sites, even over a period of less than one year at the Pump station. The microbial community dynamics was slower at the Main tunnel and Test site, presumably due to lower water flow at these locations. The microbial communities at the three tunnel locations shared many abundant taxa but were distinctly different from each other in biofilm community structure despite the relatively close geographic distance. Null-model analyses

suggested that deterministic factors had considerable influence on microbial community assembly at the tunnel sites, possibly due to specific local environmental conditions.

- Results of the mesocosms experiment indicated that stochastic factors shaped the microbial community composition during early stage of biofilm formation on concrete exposed to seawater, while deterministic forces were important over longer time intervals with time being a key factor for the turnover (compositional differences) in the biofilm communities.
- The mesocosms experiment also suggested that both presence of steel fiber reinforcement and concrete surface roughness affected the biofilm community composition, with the former being more important.
- Genes associated with the nitrogen, sulfur, iron, and manganese cycles were detected within the reconstructed MAGs from the subsea tunnel. The biofilm community harboured metabolic potential for aerobic ammonium oxidation by AOA (*Nitrosomonas*) and AOB (*Nitrosopumilus*), aerobic nitrite oxidation by NOB (*Nitrospira* and *Nitrospina*) as well as anoxic denitrification (many taxa) and anammox (*Scalindua*). Oxidation of sulfate was a rather common trait (many taxa), but the capacity for sulfate reduction was minor. The potential for iron oxidation was detected among several MAGs belonging to different taxa, with *Mariprofundus* within *Zetaproteobacteria*, being a type species. A few MAGs could also putatively reduce iron. Five *Nitrospiria* MAGs were related to *Manganitrophus noduliformans*, a recently discovered manganese oxidizer, suggesting that autotrophic manganese oxidation was occurring in the biofilm, likely contributing to formation of manganese oxides.
- A number of the microbial metabolisms (see above) can contribute to acidification, which was evident as shown by the concrete degradation measured underneath the biofilm. Aerobic oxidation of ammonia and iron release protons, and sulfur oxidation cause formation of sulfuric acid. Also biogenic manganese oxidation can contribute to acidification via subsequent abiotic reduction of manganese(IV) oxide with concomitant oxidation of iron(II). The extent of these reactions likely varied over time and space. Within the biofilm, local environments most probably provided the necessary aerobic, microaerophilic, and anoxic conditions for the different reactions. However, a limited supply of organic matter limited anaerobic reduction of sulfate to hydrogen sulfide, which distinguish the tunnel biofilm from concrete degradation in other environments such as sewers. Furthermore, the iron-oxidizing bacteria likely contributed to the observed corrosion of the reinforcing steel fibres.

6 Perspectives and future works

Fundamental research about microbial biofilms involved in degradation of concrete material in marine environment is imperative to prevent biodeterioration of sprayed reinforced concrete in subsea tunnels. Therefore, detailed studies about microbial communities and their mechanisms and interactions with different concrete materials are of great importance. Although the present work helped us to understand the complexity of concrete biodeterioration in the Oslofjord subsea tunnel and has established important facts regarding concrete biodegradation in marine environment, there is a need for further work.

Many microorganisms detected in biofilms on concrete materials could not be assigned to any known genus or species. Furthermore, major roles and activity of high abundance microorganisms are still not clear. In order to fully understand biofilm communities and their role in concrete biodeterioration, powerful molecular techniques such as gene expression and transcriptome analysis could be applied. Methodological development when it comes to sequencing goes quickly and it become more affordable which would result in much more data in the near future. Therefore, future efforts need to apply metatranscriptomics, metaproteomics or metabolomics in order to link microbial community composition more tightly with function. Further linkage between identity and activity of microbial community members could also be provided combining methods such as fluorescence in-situ hybridisation (FISH) with SEM, called Gold-FISH.

Analytical work including microsensor measurements of NO, NO_2, H_2S, and oxidation-reduction potentials within the biofilm at a µm scale would provide better insight into microbial activity at the local sites.

In order to understand biofilm formation on concrete material and their degrading activities, manipulative studies such as temporal study with mesocosms will be needed. The development of mesocosms with different concrete properties and different environmental conditions would provide more information about the microbial colonization, composition, localization and stratification of the biofilm in relation to the degrading activities over time.

Additionally, detail studies about concrete degradation rates (such as concrete petrography and mineralogical characterisation of biominerals) would be essential to fully understand complex mechanisms involved in degradation of concrete materials.

7 REFERENCES

Albertsen, M., Karst, S. M., Ziegler, A. S., Kirkegaard, R. H., & Nielsen, P. H. (2015). Back to Basics-The Influence of DNA Extraction and Primer Choice on Phylogenetic Analysis of Activated Sludge Communities. PLoS One, 10(7): e0132783.

Alexander, M., Bertron, A., & De Belie, N. (2013). Performance of Cement-Based Materials in Aggressive Aqueous Environments (Vol. 10). Springer Netherlands.

Ali, M., Wang, Z. W., Salam, K. W., Hari, A. R., Pronk, M., van Loosdrecht, M. C. M., & Saikaly, P. E. (2019). Importance of Species Sorting and Immigration on the Bacterial Assembly of Different-Sized Aggregates in a Full-Scale Aerobic Granular Sludge Plant. Environmental Science & Technology, 53(14): 8291-8301.

Anderson, M. J. (2001). A new method for non-parametric multivariate analysis of variance. Austral Ecology, 26(1): 32-46.

APHA. (1998). Standard Methods for the examination of water and wastewater,. In. Washington DC.: American Public Health Association.

Bech, P. K., Lysdal, K. L., Gram, L., Bentzon-Tilia, M., Strube, M. L., & Pupo, M. T. (2020). Marine Sediments Hold an Untapped Potential for Novel Taxonomic and Bioactive Bacterial Diversity. Msystems, 5(5): e00782-00720.

Beech, I. B., & Sunner, J. (2004). Biocorrosion: towards understanding interactions between biofilms and metals. Current Opinion in Biotechnology, 15(3): 181-186.

Behbahani, H., Nematollahi, B., & Farasatpour, M. (2011). Steel fiber reinforced concrete: A review. Proceedings of the International Conference on Structural Engineering Construction and Management (ICSECM2011). Available: http://dl.lib.mrt.ac.lk/handle/123/9505.

Berrocal, C. G., Lundgren, K., & Löfgren, I. (2013). Influence of steel fibres on corrosion of reinforcement in concrete in chloride environments: A review. 7th International Conference Fibre Concrete 2013 Proceedings.

Berrocal, C. G., Lundgren, K., & Löfgren, I. (2016). Corrosion of steel bars embedded in fibre reinforced concrete under chloride attack: state of the art. Cement and Concrete Research, 80: 69-85.

Bertron, A. (2014). Understanding interactions between cementitious materials and microorganisms: a key to sustainable and safe concrete structures in various contexts. Materials and Structures, 47(11): 1787-1806.

Besemer, K., Peter, H., Logue, J. B., Langenheder, S., Lindstrom, E. S., Tranvik, L. J., & Battin, T. J. (2012). Unraveling assembly of stream biofilm communities. Isme Journal, 6(8): 1459-1468.

Busscher, H. J., & van Der Mei, R. B. H. C. (1995). Initial microbial adhesion is a determinant for the strength of biofilm adhesion. FEMS Microbiology Letters, 128(3): 229-234.

Callahan, B. J., McMurdie, P. J., Rosen, M. J., Han, A. W., Johnson, A. J. A., & Holmes, S. P. (2016). DADA2: high-resolution sample inference from Illumina amplicon data. Nature methods, 13(7): 581-583.

Cao, L. T., Kodera, H., Abe, K., Imachi, H., Aoi, Y., Kindaichi, T., Ozaki, T., & Ohashi, A. (2015). Biological oxidation of Mn(II) coupled with nitrification for removal and recovery of minor metals by downflow hanging sponge reactor. Water Research, 68: 545-553.

Caporaso, J. G., Lauber, C. L., Walters, W. A., Berg-Lyons, D., Lozupone, C. A., Turnbaugh, P. J., Fierer, N., & Knight, R. (2011). Global patterns of 16S rRNA diversity at a depth of millions of sequences per sample. Proceedings of the National Academy of Sciences of the United States of America, 108(Suppl 1): 4516-4522.

Cayford, B.I., Jiang, G.M., Keller, J., Tyson, G. and Bond, P.L. (2017). Comparison of microbial communities across sections of a corroding sewer pipe and the effects of wastewater flooding. Biofouling, 33(9): 780-792.

Chao, A. N., Chiu, C. H., & Jost, L. (2014). Unifying Species Diversity, Phylogenetic Diversity, Functional Diversity, and Related Similarity and Differentiation Measures Through Hill Numbers. Annual Review of Ecology, Evolution, and Systematics, 45: 297-324.

Chase, J. M., Kraft, N. J. B., Smith, K. G., Vellend, M., & Inouye, B. D. (2011). Using null models to disentangle variation in community dissimilarity from variation in alpha-diversity. Ecosphere, 2(2).

Chase, J. M., & Leibold, M. A. (2009). Ecological niches. University of Chicago Press.

Chaumeil, P.-A., Mussig, A. J., Hugenholtz, P., & Parks, D. H. (2020). GTDB-Tk: a toolkit to classify genomes with the Genome Taxonomy Database. Bioinformatics, 36(6): 1925-1927.

Choi H, Koh H-W, Kim H, Chae J-C, Park S-J. (2016).Microbial community composition in the marine sediments of Jeju Island: next-generation sequencing surveys. Journal of Microbiology and Biotechnology, 26:883–890.

Cwalina, B. (2008). Biodeterioration of concrete. Acee Journal, 4:133-140.

Cwalina, B. (2014). Biodeterioration of concrete, brick and other mineral-based building materials. Understanding Biocorrosion: Fundamentals and Applications, 11: 281-312.

Daims, H., Lebedeva, E. V., Pjevac, P., Han, P., Herbold, C., Albertsen, M., Jehmlich, N., Palatinszky, M., Vierheilig, J., & Bulaev, A. (2015). Complete nitrification by Nitrospira bacteria. Nature, 528(7583): 504-509.

Dang, H., Chen, R., Wang, L., Shao, S., Dai, L., Ye, Y., Guo, L., Huang, G., & Klotz, M. G. (2011). Molecular characterization of putative biocorroding microbiota with a novel niche detection of Epsilon- and Zetaproteobacteria in Pacific Ocean coastal seawaters. Environmental Microbiology, 13(11): 3059-3074.

Dang, H., & Lovell, C. R. (2016). Microbial surface colonization and biofilm development in marine environments. Microbiology and Molecular Biology Reviews, 80(1): 91-138.

Donlan, R. M. (2002). Biofilms: Microbial life on surfaces. Emerging Infectious Diseases, 8(9): 881-890.

Dyer, T. (2017). Biodeterioration of Concrete. CRC Press by Taylor and Francis Group.

Eddy, S. R. (2011). Accelerated Profile HMM Searches. PLOS Computational Biology, 7(10): e1002195.

Edgar, R. C. (2010). Search and clustering orders of magnitude faster than BLAST. Bioinformatics, 26(19): 2460-2461.

Edgar, R. C. UPARSE (2013). highly accurate OTU sequences from microbial amplicon reads. Nature Methods, 10(10):996-998.

Edgar, R. (2016). SINTAX: a simple non-Bayesian taxonomy classifier for 16S and ITS sequences. bioRxiv. https://doi.org/10.1101/074161

Edgar, R. C. (2016). UNOISE2: improved error-correction for Illumina 16S and ITS amplicon sequencing. bioRxiv. https://doi.org/10.1101/081257

Edgar, R. C., & Flyvbjerg, H. (2015). Error filtering, pair assembly and error correction for next-generation sequencing reads. Bioinformatics, 31(21): 3476-3482.

Emerson, D., & Ghiorse, W. C. (1992). Isolation, Cultural Maintenance, and Taxonomy of a Sheath-Forming Strain of Leptothrix discophora and Characterization of Manganese-Oxidizing Activity Associated with the Sheath. Applied Environmental Microbiology, 58(12): 4001-4010.

Emerson, D., & Moyer, C. L. (2002). Neutrophilic Fe-oxidizing bacteria are abundant at the Loihi Seamount hydrothermal vents and play a major role in Fe oxide deposition. Applied Environmental Microbiology, 68(6): 3085-3093.

Ferrari, C., Santunione, G., Libbra, A., Muscio, A., Sgarbi, E., Siligardi, C., & Barozzi, G. S. (2015). Review on the influence of biological deterioration on the surface properties of building materials: organisms, materials, and methods. International Journal of Design & Nature and Ecodynamics, 10(1): 21-39.

Flemming, H.-C., Murthy, S., Venkatesan, R., & Cooksey, K. (2009). Marine and Industrial Biofouling. Springer International Publishing.

Flemming, H. C., & Wingender, J. (2010). The biofilm matrix. Nature Reviews Microbiology, 8(9): 623-633.

Flemming, H. C., Wingender, J., Szewzyk, U., Steinberg, P., Rice, S. A., & Kjelleberg, S. (2016). Biofilms: an emergent form of bacterial life. Nature Reviews Microbiology, 14(9): 563-575.

Garber, A. I., Nealson, K. H., Okamoto, A., McAllister, S. M., Chan, C. S., Barco, R. A., & Merino, N. (2020). FeGenie: A comprehensive tool for the identification of iron genes and iron gene neighborhoods in genome and metagenome assemblies. Frontiers in Microbiology, 11:37.

Gaylarde, C. (2020). Influence of Environment on Microbial Colonization of Historic Stone Buildings with Emphasis on Cyanobacteria. Heritage, 3(4): 1469-1482.

Gaylarde, C., & Morton, G. (2003). Biodeterioration of mineral materials. Encyclopedia of environmental microbiology. Wiley, 515-528.

Gaylarde, C., Silva, M. R., & Warscheid, T. (2003). Microbial impact on building materials: an overview. Materials and Structures, 36(259): 342-352.

Gomez-Alvarez, V., Revetta, R.P. and Domingo, J.W.S. (2012). Metagenome analyses of corroded concrete wastewater pipe biofilms reveal a complex microbial system. BMC Microbiology, 12:122.

Grengg, C., Mittermayr, F., Baldermann, A., Bottcher, M. E., Leis, A., Koraimann, G., Grunert, P., & Dietzel, M. (2015). Microbiologically induced concrete corrosion: A case study from a combined sewer network. Cement and Concrete Research, 77: 16-25.

Gutierrez-Padilla, M., Guadalupe, D., Bielefeldt, A., Hernandez, M., & Silverstein, J. (2007). Monitoring of microbially induced concrete corrosion in pipelines. Paper presented at the Corrosion 2007.

Hagelia, P. (2007). Sprayed concrete deterioration influenced by saline ground water and Mn- and Fe-biomineralisation in subsea road tunnels. Jamtveit, B. (ed), Mechanical effects on reactive systems. p. 26, The 20th Kongsberg Seminar, Norway.

Hagelia, P. (2011a). Deterioration mechanisms and durability of sprayed concrete for rock support in tunnels, PhD thesis, TU Delft, Delft, the Netherlands.

Hagelia, P. (2011b). Sprayed concrete in aggressive subsea environment – the Oslofjord Test Site. In: Beck T, Woldmo O, Engen S, editors. Proceedings of the 6th international symposium on sprayed concrete - Modern Use of Wet Mix Sprayed Concrete for Underground Support, Tromso, Norway.

Hagelia, P., Karačić, S., Haverkamp, T.H.A., Persson, F., & Wilén, B.-M. (2020). Biodeterioration of sprayed concrete in subsea tunnels. Investigations into the role and nature of Mn–Fe biofilm over 17 years. Microorganisms-Cementitious Materials Interactions, Chapter 4.2, RILEM TC 253-MCI State-of-the-Art-Report, Springer (in press).

Harbulakova, V.O., Estokova, A., Stevulova, N., Luptáková, A., & Foraiova, K. (2013). Current Trends in Investigation of Concrete Biodeterioration. Procedia Engineering, 65(0):346-351.

Hayek, M., Salgues, M., Souche, J.-C., Cunge, E., Giraudel, C., & Paireau, O. (2021). Influence of the Intrinsic Characteristics of Cementitious Materials on Biofouling in the Marine Environment. Sustainability, 13(5): 2625.

He Y, Caporaso JG, Jiang X-T, Sheng H-F, Huse SM, Rideout JR, et al. (2015). Stability of operational taxonomic units: an important but neglected property for analyzing microbial diversity. Microbiome, 3(1):20.

Hudon, E., Mirza, S., & Frigon, D. (2011). Biodeterioration of Concrete Sewer Pipes: State of the Art and Research Needs. Journal of Pipeline Systems Engineering and Practice, 2(2): 42-52.

Hugerth, L. W., Wefer, H. A., Lundin, S., Jakobsson, H. E., Lindberg, M., Rodin, S., Engstrand, L., & Andersson, A.F. (2014). DegePrime, a program for degenerate primer design for broad-taxonomic-range PCR in microbial ecology studies. Applied Environmental Microbiology, 80(16): 5116-5123.

Hughes, P. (2014). An investigation into marine biofouling and its influence on the durability of concrete sea defences. Doctoral thesis, University of Central Lancashire.

Hughes, P., Fairhurst, D., Sherrington, I., Renevier, N., Morton, L. H. G., Robery, P. C., & Cunningham, L. (2013). Microscopic study into biodeterioration of marine concrete. International Biodeterioration & Biodegradation, 79(0): 14-19.

Hughes, P., Fairhurst, D., Sherrington, I., Renevier, N., Morton, L. H. G., Robery, P. C., & Cunningham, L. (2014). Microbial degradation of synthetic fibre-reinforced marine concrete. International Biodeterioration & Biodegradation, 86, Part A(0): 2-5.

Hvitved-Jacobsen, T., Vollertsen, J., Yongsiri, C., Nielsen, A., & Abdul-Talib, S. (2002). Sewer microbial processes, emissions and impacts. In Proceedings from the 3rd International Conference on Sewer Processes and Networks, Paris, France, April 15-17, (pp. 1-13)

Hyatt, D., Chen, G.-L., LoCascio, P. F., Land, M. L., Larimer, F. W., & Hauser, L. J. (2010). Prodigal: prokaryotic gene recognition and translation initiation site identification. BMC Bioinformatics, 11(1): 119.

Håvelsrud OE, Haverkamp TH, Kristensen T, Jakobsen KS, Rike AG. 2012. Metagenomic and geochemical characterization of pockmarked sediments overlaying the troll petroleum reservoir in the North Sea. BMC Microbiology, 12:203

Islander, R. L., Devinny, J. S., Mansfeld, F., Postyn, A., & Shih, H. (1991). Microbial ecology of crown corrosion in sewers. Journal of Environmental Engineering, 117(6): 751-770.

Javaherdashti, R. (2017). Microbiologically Influenced Corrosion (MIC). In Microbiologically Influenced Corrosion: An Engineering Insight (pp.29-79). Springer International Publishing.

Jost, L. (2006). Entropy and diversity. OIKOS, 113(2): 363-375.

Jost, L. (2007). Partitioning diversity into independent alpha and beta components. Ecology, 88(10): 2427-2439.

Karačić, S., Hagelia, P., Haverkamp, T. H., Persson, F., & Wilén, B.-M. (2018). Biodeterioration of reinforced sprayed concrete in subsea tunnels. Final Conference of RILEM TC 253-MCI: Microorganisms-Cementitious Materials Interactions, France.

Kembel, S. W., Cowan, P. D., Helmus, M. R., Cornwell, W. K., Morlon, H., Ackerly, D. D., Blomberg, S. P., & Webb, C. O. (2010). Picante: R tools for integrating phylogenies and ecology. Bioinformatics, 26(11): 1463-1464.

Kozich, J. J., Westcott, S. L., Baxter, N. T., Highlander, S. K., & Schloss, P. D. (2013). Development of a Dual-Index Sequencing Strategy and Curation Pipeline for Analyzing Amplicon Sequence Data on the MiSeq Illumina Sequencing Platform. Applied and Environmental Microbiology, 79(17): 5112-5120.

Kulichevskaya, I. S., Ivanova, A. A., Detkova, E. N., Rijpstra, W. I. C., Sinninghe Damsté, J. S., & Dedysh, S. N. (2015). Planctomicrobium piriforme gen. nov., sp. nov., a stalked planctomycete from a littoral wetland of a boreal lake. International Journal Systematic and Evolutionary Microbiology, 65(Pt_5): 1659-1665.

Liébana, R., Modin, O., Persson, F., Szabó, E., Hermansson, M., & Wilén, B.-M. (2019). Combined deterministic and stochastic processes control microbial succession in replicate granular biofilm reactors. Environmental Science & Technology, 53(9): 4912-4921.

Little, B. J., & Lee, J. S. (2007). Microbiologically influenced corrosion (Vol. 3). John Wiley & Sons.

Little, B. J., Lee, J. S., & Ray, R. I. (2008). The influence of marine biofilms on corrosion: A concise review. Electrochimica Acta, 54(1): 2-7.

Love, M. I., Huber, W., & Anders, S. (2014). Moderated estimation of fold change and dispersion for RNA-seq data with DESeq2. Genome Biology, 15(12): 550.

Lucker, S., Nowka, B., Rattei, T., Spieck, E., & Daims, H. (2013). The Genome of Nitrospina gracilis Illuminates the Metabolism and Evolution of the Major Marine Nitrite Oxidizer. Frontiers in Microbiology, 4:27.

Lucker, S., Wagner, M., Maixner, F., Pelletier, E., Koch, H., Vacherie, B., Rattei, T., Damste, J. S., Spieck, E., Le Paslier, D., & Daims, H. (2010). A Nitrospira metagenome illuminates the physiology and evolution of globally important nitrite-oxidizing bacteria. Proceedings of the National Academy of Science U S A, 107(30): 13479-13484.

Ma, Y., Zhang, Y., Zhang, R., Guan, F., Hou, B., & Duan, J. (2020). Microbiologically influenced corrosion of marine steels within the interaction between steel and biofilms: a brief view. Applied Microbiology and Biotechnology, 104(2): 515-525.

Machuca Suarez, L. (2019). Understanding and addressing microbiologically influenced corrosion (MIC). Corrosion & Materials, 44(1): 88-96.

Magniont, C., Coutand, M., Bertron, A., Cameleyre, X., Lafforgue, C., Beaufort, S., & Escadeillas, G. (2011). A new test method to assess the bacterial deterioration of cementitious materials. Cement and Concrete Research, 41(4): 429-438.

Márquez, J. F., Sanchez-Silva, M., & Husserl, J. (2013). Review of reinforced concrete biodeterioration mechanisms. Proceeding of VIII International Conference on Fracture Mechanics of Concrete and Concrete Structures- FraMCoS-8, Toledo.

McAllister, S. M., Polson, S. W., Butterfield, D. A., Glazer, B. T., Sylvan, J. B., & Chan, C. S. (2020). Validating the Cyc2 neutrophilic iron oxidation pathway using meta-omics of Zetaproteobacteria iron mats at marine hydrothermal vents. Msystems, 5:e00553-19

McBeth, J.M., Little, B.J., Ray, R.I., Farrar, K.M. and Emerson, D. (2011). Neutrophilic iron-oxidizing Zetaproteobacteria and mild steel corrosion in nearshore marine environments. Applied Environmental Microbiology, 77(4): 1405-1412.

McBeth JM, Emerson D. (2016). In situ microbial community succession on mild steel in estuarine and marine environments: exploring the role of iron-oxidizing bacteria. Frontiers Microbiology. 7:767.

McIlroy, S. J., Saunders, A. M., Albertsen, M., Nierychlo, M., McIlroy, B., Hansen, A. A., Karst, S. M., Nielsen, J. L., & Nielsen, P. H. (2015). MiDAS: the field guide to the microbes of activated sludge. Database (Oxford), 2015, bav062.

Mehta, P. K., & Monteiro, P. J. (2014). Concrete: microstructure, properties, and materials. McGraw-Hill Education.

Miller, A. Z., Sanmartin, P., Pereira-Pardo, L., Dionisio, A., Saiz-Jimenez, C., Macedo, M. F., & Prieto, B. (2012). Bioreceptivity of building stones: a review. Science of the Total Environment, 426: 1-12.

Modin, O., Liebana, R., Saheb-Alam, S., Wilen, B. M., Suarez, C., Hermansson, M., & Persson, F. (2020). Hill-based dissimilarity indices and null models for analysis of microbial community assembly. Microbiome, 8(1): 1-16.

Monteny, J., De Belie, N., Vincke, E., Verstraete, W., & Taerwe, L. (2001). Chemical and microbiological tests to simulate sulfuric acid corrosion of polymer-modified concrete. Cement and Concrete Research, 31(9): 1359-1365.

Nica, D., Davis, J., Kirby, L., Zuo, G., & Roberts, D. (2000). Isolation and characterization of microorganisms involved in the biodeterioration of concrete in sewers. International Biodeterioration & Biodegradation, 46(1): 61-68.

Noeiaghaei, T., Mukherjee, A., Dhami, N., & Chae, S.-R. (2017). Biogenic deterioration of concrete and its mitigation technologies. Construction and Building Materials, 149: 575-586.

Ogawa, A., Tanaka, R., Hirai, N., Ochiai, T., Ohashi, R., Fujimoto, K., Akatsuka, Y., & Suzuki, M. (2020). Investigation of Biofilms Formed on Steelmaking Slags in Marine Environments for Water Depuration. International Journal of Molecular Sciences, 21(18): 6945.

Okabe, S., Odagiri, M., Ito, T., & Satoh, H. (2007). Succession of sulfur-oxidizing bacteria in the microbial community on corroding concrete in sewer systems. Applied and Environmental Microbiology, 73(3): 971-980.

Oksanen J, B. F., Friendly M, Kindt R, Legendre P, McGlinn D, et al. (2017). vegan: Community Ecology Package.

Park, B. J., Park, S. J., Yoon, D. N., Schouten, S., Sinninghe Damste, J. S., & Rhee, S. K. (2010). Cultivation of autotrophic ammonia-oxidizing archaea from marine sediments in coculture with sulfur-oxidizing bacteria. Applied Environmental Microbiology, 76(22): 7575-7587.

Parks, D. H., Chuvochina, M., Chaumeil, P.-A., Rinke, C., Mussig, A. J., & Hugenholtz, P. (2020). A complete domain-to-species taxonomy for Bacteria and Archaea. NatureBiotechnology, 38(9): 1079-1086.

Parks, D. H., Chuvochina, M., Waite, D. W., Rinke, C., Skarshewski, A., Chaumeil, P.-A., & Hugenholtz, P. (2018). A standardized bacterial taxonomy based on genome phylogeny substantially revises the tree of life. Nature Biotechnology, 36(10): 996-1004.

Percival, S. L., Knapp, J. S., Wales, D. S., & Edyvean, R. G. J. (1999). The effect of turbulent flow and surface roughness on biofilm formation in drinking water. Journal of Industrial Microbiology and Biotechnology, 22(3): 152-159.

Permeh, S., Boan, M. E., Tansel, B., & Lau, K. (2019). Susceptibility of bridge steel and concrete components to microbiological influenced corrosion (MIC) and microbiological influenced deterioration (MID) in Florida marine environment: A case study. In Proceedings of the Corrosion 2017, LA.

Peyre-Lavigne, M., Bertron, A., Auer, L., Hernandez-Raquet, G., Foussard, J.-N., Escadeillas, G., Cockx, A., & Paul, E. (2015). An innovative approach to reproduce the biodeterioration of industrial cementitious products in a sewer environment. Part I: Test design. Cement and Concrete Research, 73(0): 246-256.

Peyre-Lavigne, M., Lors, C., Valix, M., Herisson, J., Paul, E., & Bertron, A. (2016). Microbial induced concrete deterioration in sewers environment: mechanisms and microbial populations. RILEM TC 253 MCI Proceedings, Delft, the Netherland, 20-36.

Procópio, L. (2020). Microbial community profiles grown on 1020 carbon steel surfaces in seawater-isolated microcosm. Annals of Microbiology, 70(1):13.

Quast, C., Pruesse, E., Yilmaz, P., Gerken, J., Schweer, T., Yarza, P., Peplies, J., & Glöckner, F. O. (2012). The SILVA ribosomal RNA gene database project: improved data processing and web-based tools. Nucleic Acids Research, 41(D1): D590-D596.

R Core Team. (2020). R: A language and environment for statistical computing. https://www.R-project.org/

Raup, D. M., & Crick, R. E. (1979). Measurement of Faunal Similarity in Paleontology. Journal of Paleontology, 53(5): 1213-1227.

Redford, A. J., & Fierer, N. (2009). Bacterial Succession on the Leaf Surface: A Novel System for Studying Successional Dynamics. Microbial Ecology, 58(1): 189-198.

Roberts, D. J., Nica, D., Zuo, G., & Davis, J. L. (2002). Quantifying microbially induced deterioration of concrete: initial studies. International Biodeterioration & Biodegradation, 49(4): 227-234.

Rognes, T., Flouri, T., Nichols, B., Quince, C., & Mahé, F. (2016). VSEARCH: a versatile open source tool for metagenomics. PeerJ, 4:e2584.

Sanchez-Silva, M., & Rosowsky, D. V. (2008). Biodeterioration of construction materials: State of the art and future challenges. Journal of Materials in Civil Engineering, 20(5): 352-365.

Sand, W., & Bock, E. (1991). Biodeterioration of mineral materials by microorganisms-biogenic sulfuric and nitric acid corrosion of concrete and natural stone. Geomicrobiology Journal, 9(2-3): 129-138.

Satoh, H., Odagiri, M., Ito, T., & Okabe, S. (2009). Microbial community structures and in situ sulfate-reducing and sulfur-oxidizing activities in biofilms developed on mortar specimens in a corroded sewer system. Water Research, 43(18): 4729-4739.

Schmid, M. C., Risgaard-Petersen, N., van de Vossenberg, J., Kuypers, M. M., Lavik, G., Petersen, J., Hulth, S., Thamdrup, B., Canfield, D., Dalsgaard, T., Rysgaard, S., Sejr, M. K., Strous, M., den Camp, H. J., & Jetten, M. S. (2007). Anaerobic ammonium-oxidizing bacteria in marine environments: widespread occurrence but low diversity. Environmental Microbiology, 9(6): 1476-1484.

Schüler, D., & Frankel, R. B. (1999). Bacterial magnetosomes: microbiology, biomineralization and biotechnological applications. Applied Microbiology and Biotechnology, 52(4): 464-473.

Shade, A., Caporaso, J. G., Handelsman, J., Knight, R., & Fierer, N. (2013). A meta-analysis of changes in bacterial and archaeal communities with time. ISME Journal, 7(8): 1493-1506.

Shi, L., Fredrickson, J. K., & Zachara, J. M. (2014). Genomic analyses of bacterial porin-cytochrome gene clusters. Frontiers in Microbiology, 5:657.

Simões, T., Costa, H., Dias-da-Costa, D., & Júlio, E. (2017). Influence of fibres on the mechanical behaviour of fibre reinforced concrete matrixes. Construction and Building Materials, 137: 548-556.

Soleimani, S., Isgor, O. B., & Ormeci, B. (2013). Resistance of biofilm-covered mortars to microbiologically influenced deterioration simulated by sulfuric acid exposure. Cement and Concrete Research, 53: 229-238.

Stegen, J. C., Lin, X. J., Konopka, A. E., & Fredrickson, J. K. (2012). Stochastic and deterministic assembly processes in subsurface microbial communities. Isme Journal, 6(9): 1653-1664.

Stewart, P. S. (2003). Diffusion in Biofilms. Journal of Bacteriology, 185(5): 1485-1491.

Stoodley, P., Boyle, J. D., DeBeer, D., & Lappin-Scott, H. M. (1999). Evolving perspectives of biofilm structure. Biofouling, 14(1): 75-90.

Storesund, J. E., & Øvreås, L. (2013). Diversity of Planctomycetes in iron-hydroxide deposits from the Arctic Mid Ocean Ridge (AMOR) and description of Bythopirellula goksoyri gen. nov., sp. nov., a novel Planctomycete from deep sea iron-hydroxide deposits. Antonie van Leeuwenhoek, 104(4): 569-584.

Theron, J., & Cloete, T. E. (2000). Molecular techniques for determining microbial diversity and community structure in natural environments. Critical Reviews in Microbiology, 26(1): 37-57.

Torres-Luque, M., Bastidas-Arteaga, E., Schoefs, F., Sánchez-Silva, M., & Osma, J. F. (2014). Non-destructive methods for measuring chloride ingress into concrete: State-of-the-art and future challenges. Construction and Building Materials, 68: 68-81.

Trejo, D., de Figueiredo, P., Sanchez, M., Gonzalez, C., Wei, S., & Li, L. (2008). Analysis and assessment of microbial biofilm-mediated concrete deterioration. Technical Report, U.S. Department of Transportation.

Urakawa, H., Kurata, S., Fujiwara, T., Kuroiwa, D., Maki, H., Kawabata, S., Hiwatari, T., Ando, H., Kawai, T., Watanabe, M., & Kohata, K. (2006). Characterization and quantification of ammonia-oxidizing bacteria in eutrophic coastal marine sediments using polyphasic molecular approaches and immunofluorescence staining. Environmental Microbiology, 8(5), 787-803.

Vanysacker, L., Declerck, S. A., Hellemans, B., De Meester, L., Vankelecom, I., & Declerck, P. (2010). Bacterial community analysis of activated sludge: an evaluation of four commonly used DNA extraction methods. Applied Microbiology and Biotechnology, 88(1): 299-307.

Veach, A. M., Stegen, J. C., Brown, S. P., Dodds, W. K., & Jumpponen, A. (2016). Spatial and successional dynamics of microbial biofilm communities in a grassland stream ecosystem. Molecular Ecology, 25(18): 4674-4688.

Wang, Q., Garrity, G.M., Tiedje, J.M., and Cole, JR. (2007) Naive Bayesian classifier for rapid assignment of rRNA sequences into the new bacterial taxonomy. Applied and Environmental Microbiology, 73(16):5261-5267.

Webb, C. O., Ackerly, D. D., McPeek, M. A., & Donoghue, M. J. (2002). Phylogenies and Community Ecology. Annual Review of Ecology and Systematics, 33(1): 475-505.

Wei, S., Sanchez, M., Trejo, D., & Gillis, C. (2010). Microbial mediated deterioration of reinforced concrete structures. International Biodeterioration & Biodegradation, 64(8): 748-754.

Wei, S. P., Jiang, Z. L., Liu, H., Zhou, D. S., & Sanchez-Silva, M. (2013). Microbiologically induced deterioration of concrete - A Review. Brazilian Journal of Microbiology, 44(4): 1001-1007.

Widder, S., Allen, R. J., Pfeiffer, T., Curtis, T. P., Wiuf, C., Sloan, W. T., Cordero, O. X., Brown, S. P., Momeni, B., & Shou, W. (2016). Challenges in microbial ecology: building predictive understanding of community function and dynamics. ISME Journal, 10(11): 2557-2568.

Wilén, B.-M., Persson, F., & Hagelia, P. (2014). Final report of the preliminary study of the project ”The role of microbiological biofilm communities for degradation of sprayed concrete in subsea tunnels”.

Woodcock, S., Besemer, K., Battin, T. J., Curtis, T. P., & Sloan, W. T. (2013). Modelling the effects of dispersal mechanisms and hydrodynamic regimes upon the structure of microbial communities within fluvial biofilms. Environmental Microbiology, 15(4): 1216-1225.

Wu, M., Wang, T., Wu, K., & Kan, L. (2020). Microbiologically induced corrosion of concrete in sewer structures: A review of the mechanisms and phenomena. Construction and Building Materials, 239: 117813.

Zhang, L., De Schryver, P., De Gusseme, B., De Muynck, W., Boon, N., & Verstraete, W. (2008). Chemical and biological technologies for hydrogen sulfide emission control in sewer systems: a review. Water Research, 42(1-2): 1-12.

Zhou, J., & Ning, D. (2017). Stochastic community assembly: does it matter in microbial ecology? Microbiology and Molecular Biology Reviews, 81(4): e00002-00017.